Title:

Novel class of OTU deubiquitinases regulate substrate ubiquitination upon *Legionella* infection

Authors: Donghyuk Shin[1,2,3], Anshu Bhattacharya[1,2], Yi-Lin Cheng[1,2], Marta Campos Alonso[2], Ahmad Reza Mehdipour[3], Gerbrand J. van der Heden van Noort[4], Huib Ovaa[4], Gerhard Hummer[3,5] and Ivan Dikic[1,2,3, *]

Affiliations:

[1] Institute of Biochemistry II, Faculty of Medicine, Goethe University Frankfurt, Theodor-Stern-Kai 7, 60590 Frankfurt am Main, Germany.

[2] Buchmann Institute for Molecular Life Sciences, Goethe University Frankfurt, Max-von-Laue-Str. 15, 60438 Frankfurt am Main, Germany.

[3] Max Planck Institute of Biophysics, Max-von-Laue-Str. 3, 60438 Frankfurt am Main, Germany

[4] Oncode Institute and Department of Chemical Immunology, Leiden University Medical Centre, Einthovenweg 20, 2333 ZC, Leiden, The Netherlands

[5] Institute of Biophysics, Goethe University Frankfurt, Frankfurt am Main, Germany.

*Correspondence & Lead contact: dikic@biochem2.uni-frankfurt.de

Abstract: *Legionella pneumophila* is a gram-negative pathogenic bacterium that causes Legionaries' disease. The *Legionella* genome codes more than 300 effector proteins able to modulate host-pathogen interactions during infection. Among them are also enzymes altering the host-ubiquitination system including bacterial ligases and deubiquitinases. In this study, based on homology-detection screening on 305 *Legionella* effector proteins, we identified two ***L****egionella* **OT**U-like deubiquitinases (**LOT**; LotB (Lpg1621/Ceg23) and LotC (Lpg2529), LotA (Lpg2248/Lem21) is already known). A crystal structure of LotC catalytic core ($LotC_{14-310}$) was determined at 2.4 Å and compared with other OTU deubiquitinases, including LotB. Unlike the classical OTU-family, the structures of *Legionella* OTU-family (LotB and LotC) shows an extended helical lobe between the Cys-loop and the variable loop, which define a novel class of OTU-deubiquitinase. Despite structural differences in their helical lobes, both LotB and LotC interact with ubiquitin. LotB has an additional ubiquitin binding site (S1') enabling specific cleavage of Lys63-linked poly-ubiquitin chains. By contrast, LotC only contains the S1 site and cleaves different species of ubiquitin chains. MS analysis of catalytically inactive LotB and LotC identified different categories of host-substrates for these two related DUBs. Together, our results provide new structural insights of bacterial OTU deubiquitinases and indicate distinct roles of bacterial deubiquitinases in host-pathogen interactions.

Keywords: bacterial deubiquitinase, *Legionella pneumophila,* effector proteins, OTU-deubiquitinases, ubiquitin

INTRODUCTION

Ubiquitination, a well-studied post-translational modification system, regulates the fate of various substrates by tagging them with ubiquitin (Yau and Rape, 2016). A representative example of ubiquitin-mediated cellular process is the ubiquitin-proteasome system (UPS), where misfolded proteins get ubiquitinated and degraded by the proteasome, and recycled (Dikic, 2017). For the larger cellular wastes, such as cellular components (ER, mitochondria etc.), protein aggregates or intracellular bacteria, ubiquitination works together with the autophagy machinery, which includes sequestration of ubiquitinated components and their transfer into the lysosome for degradation (Pohl and Dikic, 2019). To maintain homeostasis in the cell, ubiquitination events are tightly regulated by a reverse process called deubiquitination, where ubiquitin molecules from target substrates are specifically cleaved and recycled by deubiquitinating enzymes (deubiquitinases; DUBs) (Clague et al., 2019).

To date, about 100 different deubiquitinases (DUBs) have been identified from human. They are categorized into seven different classes, based on their structure and mechanism of actions including USP, JAMM (MPN), OTU, MJD (Josepin), UCH and the recently discovered MINDY and ZUFSP (Abdul Rehman et al., 2016; Clague et al., 2019; Haahr et al., 2018; Hermanns et al., 2018; Hewings et al., 2018; Kwasna et al., 2018). Six of them belong to the cysteine protease family (USP, OTU, MJD(Josepin), UCH, MINDY and ZUFSP), while JAMM (MPN) belongs to the zinc-containing metalloproteases. Among them, the OTU-family is distinguished from other DUBs, as they exhibit linkage specificity (Mevissen et al., 2016, 2013; Mevissen and Komander, 2017). For example, Cezanne specifically cleaves Lys11-linked polyubiquitin chains (Bremm et al., 2010) and OTUB1 preferentially cleaves Lys48-linked chains (Edelmann et al., 2009; Wang et al., 2009), while OTULIN exclusively cleaves M1-linked (linear)

63 chains (Keusekotten et al., 2013). Extensive biochemical and structural studies have provided
64 general mechanisms of how the diverse linkage specificity can be achieved within the structurally
65 similar OTU-family, pointing to the presence or absence of additional ubiquitin binding domains
66 (UBDs), sequence variations on ubiquitinated substrates, or additional S1'/S2 binding sites
67 (Mevissen et al., 2013).

68 Considering the importance of ubiquitin-mediated cellular pathways, it is not surprising
69 that pathogens are armed with various weapons to hijack the host-ubiquitination system. For
70 instance, *Salmonella typhimurium* encodes HECT type E3 ligase SopA (Diao et al., 2008; Fiskin
71 et al., 2017; Lin et al., 2012) and *Legionella pneumophila* contains LubX and LegU1, which are
72 similar to U-box and F-box containing E3 ligases, respectively (Ensminger and Isberg, 2010;
73 Kubori et al., 2008; Quaile et al., 2015). In addition, bacterial pathogens also possess atypical
74 ubiquitin ligases that do not belong to any of known E3 ligases, such as IpaH family (*Shigella*) or
75 SidC/SdCA (*Legionella*) (Hsu et al., 2014; Wasilko et al., 2018). More recently, the SidE family
76 (SdeA, SdeB, SdeC and SidC) of *Legionella* has been shown to mediate unconventional
77 phosphoribosyl (PR) serine ubiquitination which is also tightly regulated by the meta-effector SidJ
78 or PR-ubiquitin specific deubiquitinases (DupA and DupB) (Bhogaraju et al., 2019, 2016; Black
79 et al., 2019; Kalayil et al., 2018; Qiu et al., 2016; Shin et al., 2020). Pathogenic bacteria encode
80 not only ubiquitin ligases, but also deubiquitinases (Hermanns and Hofmann, 2019). The most
81 studied bacterial deubiquitinases are CE-clan proteases, based on the MEROPS database
82 classification, which cleave either ubiquitin or ubiquitin-like modifiers (SUMO1 or NEDD8)
83 (Pruneda et al., 2016; Rawlings et al., 2018). In addition to CE-clan DUBs, bacteria and viruses
84 also encode OTU-like deubiquitinases. Several structures from viral-OTUs revealed that they have
85 a unique structure compared to those of known OTU family members (Akutsu et al., 2011;

86 Capodagli et al., 2013; James et al., 2011; Lombardi et al., 2013; van Kasteren et al., 2013). OTUs
87 from nairovirus Crimean-Congo hemorrhagic fever virus (CCHFV) and Dugbe virus (DUGV)
88 have an extra β-hairpin in their S1 binding site. Papain-like protease (PLP2) domain of the
89 artervirus equine arteritis virus (EAV) contains a zinc-finger that also interacts with ubiquitin.
90 While viral OTUs have been studied, to date only three bacterial OTU-like DUBs have been
91 identified. ChlaOTU from *Chlamydophila pneumoniae* contains an OTU-domain that cleaves both
92 K48- and K63-linked polyubiquitin chains (Furtado et al., 2013). LotA (Lpg2248;Lem21),
93 ***L**egionella* **OT**U-like deubiquitinase, contains two OTU-like domains with two catalytic Cys
94 residues (C13, C303), where both are required for cleaving ubiquitin chains from an LCV
95 (*Legionella*-containing vacuole) (Kubori et al., 2018). Interestingly, LotA showed K6-linkage
96 preference that is solely dependent on its first OTU domain (Cys13). Recently, another OTU-like
97 deubiquitinase from *Legionella* (Lpg1621, Ceg23) has been identified as K63 chain-specific OTU-
98 deubiquitinase (Ma et al., 2020).

99 Despite these findings, little is known about the structure and molecular details of bacterial
100 OTU-like deubiquitinases. Here, we describe the two novel OTU-like deubiquitinaseses in
101 *Legionella* (LotB (Lpg1621; Ceg23) and LotC (Lpg2529). Structural analysis on LOT-
102 deubiqutinases provides insights on how bacterial OTU-deubiquitnases distinguished from the
103 known OTU members. Furthermore, we also identified the specific host-substrates of LotB and
104 LotC by mass-spectrometry (MS) analysis using catalytically inactive variants. Collectively, our
105 findings provide valuable structural insights into bacterial deubiquitinases and their roles in host-
106 pathogen interactions.

107

108 **RESULTS**

109 **Identification of two novel OTU-like deubiquitinases from *Legionella* effector proteins**

110 To identify putative deubiquitinases amongst *Legionella* effector proteins, we analyzed effector
111 proteins from *L. pneumophlia* (Lpg genes). Based on the type IV Icm/Dot complex secretion signal
112 (> 2.0), 305 effector proteins were selected (Burstein et al., 2016). Using pairwise sequence-
113 structure comparison based on hidden Markov models (HMMs, HHpred suite) (Zimmermann et
114 al., 2018), revealed four previously uncharacterized proteins as putative deubiquitinases. These
115 proteins all contain catalytic domains of known deubiquitinases (Fig. 1a). Lpg1621(Ceg23) and
116 Lpg2529 are found as members of OTU-family, whereas Lpg2411 and Lpg2907 belong to the
117 UCH and CE-clan, respectively (Fig. 1b, Table 1). An *in vitro* di-ubiquitin cleavage assay with di-
118 Ub panel (eight different linkage-specific Ub_2 chains(El Oualid et al., 2010)) showed that the OTU-
119 like DUBs (Lpg1621 and Lpg2529) are capable of cleaving Ub_2 chains with different specificity,
120 while other candidates (Lpg2411 and Lpg2907) did not show catalytic activity (Supplementary
121 Fig. 1a). The OTU family deubiquitinases have been shown to have linkage specificity against
122 certain polyubiquitin chains (Mevissen et al., 2016, 2013). To address whether Lpg1621 and
123 Lpg2529 follow this fundamental rule, we performed a time-course *in vitro* DUB assay with di-
124 Ub panel (Fig. 1c-f). Consistent with the recent evidence, Lpg1621 exclusively processed the K63-
125 linked Ub_2 (Ma et al., 2020), while Lpg2529 showed activity against K6-, K11-, K33-, K48- and
126 K63- linked Ub_2. Based on the sequence homology and catalytic activity, we now re-named the
127 Lpg1621 and Lpg2529 as ***L**egionella* **OT**U-like deubiquitinases (LotB and LotC, respectively).

128

129 **Biochemical properties of LotB and LotC**

130 The OTU-family belongs to the cysteine protease family, requiring the presence of a catalytic triad
131 for their activity (Mevissen et al., 2013). Based on the sequence analysis, we identifed the

132 conserved catalytic triad for both LotB (D27, C29 and H270) and LotC (D17, C24 and H304).
133 Mutations on either cysteine or histidine completely abolished the catalytic activity of both DUBs,
134 which suggests that both LotB and LotC follow the general catalytic mechanism of the OTU-
135 family (Fig. 2a, c). Next, we sought to find whether LotB and LotC require additional ubiquitin
136 binding sites (S1' or S2). To elicit this information, we used two different types of ubiquitin
137 activity-based probes (ABP). The propargyl-ubiquitin-ABP (Prg-ABP) contains a highly reactive
138 propargyl group at the C-terminus of ubiquitin chains, which can form a covalent bond with the
139 catalytic cysteine (Ekkebus et al., 2013; Flierman et al., 2016; Sommer et al., 2013). The
140 vinylmethylester-ubiquitin-ABP (VME-ABP) contains VME, which replaces the isopeptide bond
141 between two ubiquitin moieties in chains, and also forms a covalent bond with the catalytic
142 cysteine (Borodovsky et al., 2002; Mulder et al., 2014). Both LotB and LotC showed clear shifts
143 with all Prg-ABPs (mono-, K48- and K63- linked) with different reactivity. LotB shifted after 30
144 mins, and only partially, as evident by the amount of unreacted species, while LotC has rapidly
145 reacted with Prg-ABP and was completely conjugated after 30 minutes (Fig. 2d, e). These results
146 suggest that both LotB and LotC have a primary ubiquitin binding S1 site where the propargyl
147 group can be located in close proximity to the catalytic cysteine. In contrast with Prg-ABP, only
148 LotB reacted with K63-Ub_2-VME-ABP. This is consistent with the di-Ub panel assay (Fig. 1c-f),
149 in which LotB showed specificity toward the K63-linkage. The VME-ABp results suggest an extra
150 S1' ubiquitin binding site on LotB, which helps to properly locate the K63-linked-VME group on
151 the catalytic site proximal to the catalytic cysteine. LotC lacks this S1' site so that VME group
152 between two ubiquitin moieties cannot be reached to the catalytic cysteine. Next, we asked whether
153 both LotB and LotC can also interact with other ubiquitin-like modifiers (SUMO1/2/3, NEDD8)
154 (Fig. 2f, g, Supplementary Fig. 2a, b). Interestingly, LotB showed modification with both NEDD8-

155 Prg and ubiquitin-Prg after 30 minutes of reaction, while LotC was modified only with ubiquitin.
156 It suggests that LotB binds to ubiquitin through the conserved binding interface with NEDD8,
157 while LotC interacts with ubiquitin through the specific residues present only in ubiquitin
158 (Supplementary Fig. 2c).
159

160 **Structural analysis of *Legionella* OTU-like deubiquitinases**

161 Linkage specificity of the OTU family relies on one of the following mechanisms: 1) additional
162 ubiquitin-binding domains, 2) ubiquitinated sequences in the substrates or 3) defined S1' or S2
163 ubiquitin-binding sites (Mevissen et al., 2013). To define the minimal OTU domain for
164 biochemical and structural studies, we designed several constructs and tested their activity against
165 the di-Ub panel (Fig. 3a, b). While LotC retained its activity with the predicted OTU domain (7-
166 310), LotB lost its activity after deletion of 50 amino acids (300-350) located at the C-terminus
167 beyond the predicted OTU domain (11-283). Based on the LotB structure (PDB:6KS5, (Ma et al.,
168 2020)), we assumed that this extra helical region might be required for the additional ubiquitin
169 binding site (S1') to accept the distal ubiquitin moiety from K63 Ub_2 (Fig. 3c). To understand the
170 detailed mechanism of linkage specificity of LotB and LotC at the molecular level, we determined
171 the crystal structure of the catalytic domain of LotC ($LotC_{14-310}$) at 2.4 Å (Fig. 3d, Supplementary
172 Table 1, PDB ID: 6YK8). A structural comparison of both LotB and LotC with other OTU-
173 deubiquitinases predicted by HHpred revealed that both Lot-DUBs have the unique structural
174 features in the S1 ubiquitin-binding site (Fig. 3c, d and Table 1). Whereas the overall fold of the
175 catalytic core of LotB and LotC resembles that of other OTU-deubiquitinases, both showed clear
176 differences in the helical arm region, which has been shown to interact with ubiquitin and it serves
177 as an S1 binding site (Mevissen et al., 2013). The structure and sequence alignment with other

178 OTUs clearly showed that both LotB and LotC contain a relatively long insertion between the Cys-
179 loop and the variable loop, compared to other OTU members (Fig. 3e). The typical length of the
180 helical lobe of the known OTUs is ranging from 50 to 60 amino acids (except Otubain family
181 which contain 110-120 amino acids), while LotB and LotC contain 183 and 210 amino acids,
182 respectively. Based on this observation, we wondered whether LotA, another *Legionella* OTU-
183 deubiquitinase (Kubori et al., 2018), also contains a longer insertion in the same region. Based on
184 the catalytic cysteine and histidine residues of the two OTU domains on LotA (Hermanns and
185 Hofmann, 2019), we analyzed the sequence and found that both OTU domains of LotA also contain
186 the longer insertion between the Cys loop and the variable loop (179 and 178 amino acids,
187 respectively; Fig. 3e). Together, our results identify Lot-DUBs as a novel class of the OTU-family
188 with longer insertions in the helical lobe region (Supplementary Fig.3a).
189

190 **Novel structural fold of S1-ubiquitin binding sites on *Legionella* OTUs**

191 Both LotB and LotC have extended helices, specifically near the S1 ubiquitin binding site and we
192 wondered how these regions interact with ubiquitin. To address this, we performed ubiquitin
193 docking into both LotB and LotC, followed by molecular dynamics (MD) simulations for 600 ns
194 (Fig. 4a-d). The final models showed that ubiquitin indeed makes contacts with the additional
195 helical regions of both LotB and LotC. In LotB, Phe143 and Met144 make hydrophobic
196 interactions with ubiquitin (Phe45 and Ala46). In addition to these interactions, we also found
197 another hydrophobic patch in LotB (Ile238, Val247, Ala248, Ile264, Ala266) interacting with
198 ubiquitin (Leu71, Leu73). For LotC, we identified several hydrophobic interactions of the
199 extended helical region (Tyr119, Tyr149) with ubiquitin (Ile44). During the simulation, C-
200 terminus of ubiquitin (Arg72, Arg74) formed transient electrostatic interactions with LotC

201 (Glu153, Glu245). To validate the interactions observed in the simulations, we introduced several
202 mutations to the binding interface of both LotB and LotC, and performed a ubiquitin-cleavage
203 assay (Fig.4e, f). Consistent with a recent study(Ma et al., 2020), mutations of both F143 and M144
204 decreased the catalytic activity of LotB. Interestingly, mutations of the newly identified
205 hydrophobic patch (I238, A266) also decreased the catalytic activity. For LotC, the mutations in
206 the hydrophobic patch (Y119, Y149) also affected the catalytic activity of LotC. Remarkably, a
207 single mutation on E153 completely abolished the catalytic activity, which indicates that the
208 electrostatic interactions are important for the correct docking of the ubiquitin C-terminus to the
209 catalytic pocket of LotC. This observation also explains the result observed in ubiquitin-like
210 protein ABP assays with LotC (Fig. 2g). The NEDD8, which has alanine instead of Arg72 in
211 ubiquitin, showed no modification towards LotC (Supplementary Fig. 2c). Together, our results
212 reveal how the extra helical lobes of the Lot-DUBs interact with ubiquitin and how they differ
213 within the *Legionella* OTU family.
214
215 **Physiological roles of LotB and LotC**
216 To gain better insights into the physiological roles of LotB and LotC, we decided to identify their
217 interacting proteins or substrates. First, to enrich for the interacting partners, catalytically inactive
218 LotB or LotC were expressed in cells and immuno-precipitated from cell lysates. Ubiquitin
219 (UBA52) is strongly enriched with both catalytically inactive LotB and LotC (Fig. 5a, c). MS
220 analysis revealed that LotB mainly interacts with membrane protein complexes (COPB1, ATP5B,
221 ATP5H, COX5A, SEC61B). We also found interactions with some ER-resident proteins (Calnexin
222 (CANX), DDOST, STT3A). By contrast, most of the enriched proteins from the inactive LotC
223 pull-down were non-membrane-bound organelle- and ribosome-related proteins (RPS8, RPLP2,

224 RPS27, RPLP1, RPL13) (Fig. 5a, c). To further understand this, we sought to find the cellular
225 localization of both DUBs (Fig. 5b, d). Consistent with the recent publication, LotB specifically
226 co-localized with the ER marker protein Calnexin, but not with other organelle markers (TOMM20
227 and GM130 for Mitochondria and Golgi, respectively, Fig. 5b), and the OTU domain itself failed
228 to localize on the ER (Supplementary Fig. 4a). By contrast, we could not find a specific cellular
229 localization of LotC (Fig. 5d). Next, to gain more insights into the functional roles of LotB and
230 LotC, we decided to explore combinatorial ubiquitination events with other ubiquitin-related
231 *Legionella* effector proteins. To do this, we co-transfected the cells with one of the Lot-DUBs and
232 previously known *Legionella* E3 ligases (SidC or SdcA) (Hsu et al., 2014; Wasilko et al., 2018).
233 We chose these two ligases because their cellular substrates are poorly studied. TMT-labelled
234 samples from cells expressing either SidC or SdcA alone, or together with a catalytically inactive
235 mutant of LotB or LotC, were prepared (four combinations; SidC-LotB, SidC-LotC, SdcA-LotC
236 or SdcA-LotC, Fig. 5e, f, Supplementary Fig. 5a-d). Interestingly, we identified a distinct sub-
237 class of substrates. Overall, a smaller number of proteins were enriched with LotB compared to
238 LotC. We reasoned that LotB specifically interacts with proteins modified with K63-linked
239 ubiquitin chains, while LotC interacts with different types of ubiquitin chains. Intriguingly, we
240 found a significant number of ribosome-structural proteins in LotC:SdcA combination, which were
241 not enriched in SidC background. Together, these results provide fundamental insights into how
242 *Legionella*-derived E3-ligases and DUBs interact with each other.
243

244 **DISCUSSION**

245 In this study, we have identified two novel bacterial OTU-deubiquitinases from *Legionella*,
246 which we suggest as founding members of a new sub-class. Unlike classical OTU-DUBs, the

247 *Legionella* OTU-DUBs (LOT) possess extended helical insertions between the catalytic Cys-loop
248 and the variable loop. Molecular dynamic simulations with biochemical studies showed that the
249 helical insertions interact with ubiquitin. As this insertion is unique for *Legionella* OTUs and not
250 found in other known OTU-family members, *Legionella* OTU-DUBs define a new sub-class of
251 the OTU-deubiquitinase family. We have also shown that LotB and LotC are specific to certain
252 ubiquitin chains and have a distinct cellular localization. Moreover, host-protein interactome
253 studies revealed that LotB and LotC have different sets of host-interacting proteins to LotB and
254 LotC. Together, these findings establish important guidance on how to screen for more DUBs in
255 other pathogenic bacteria or viruses, how to characterize their physiological roles during infection.
256 We also showed that the two *Legionella* OTUs have different ubiquitin-binding modes
257 that enable them to cleave specific ubiquitin chains. With ubiquitin activity-based probes (Prg-,
258 VME- probes), we showed that LotB contains an extra ubiquitin-binding site (S1') and is specific
259 to K63-linked ubiquitin chains, wherease LotC cleaves different types of ubiquitin chains.
260 Interestingly, we observed a modification of LotB with NEDD8-Prg ABP. Further studies on
261 neddylated proteins with LotB will give us more insights into dual-activity of LotB. In contrast,
262 we could not see the modification between NEDD8-ABP and LotC and we reasoned that the Arg72
263 on ubiquitin, which is replaced by alanine in NEDD8, is important to locate the C-terminus of
264 ubiquitin to the catalytic site. Indeed, in molecular dynamic simulations of LotC with ubiquitin we
265 found Arg72 to from transient interactions with Glu153 of LotC. Further structural analysis will
266 shed light on how different ubiquitin chains bind to LotB or LotC through the different binding
267 modes should give us further insights.
268 Deubiquitinases from bacteria and viruses have been shown to alter the host immune
269 system. For example, papain-like proteases (PLPro) from coronaviruses, such as middle east

270 respiratory syndrome (MERS) or severe acute respiratory syndrome (SARS) have dual
271 deubiquitinase and de-ISGylation activities and antagonized type I interferon (IFN-I) response,
272 which is the primary defense system against viral infections (Davis and Gack, 2015; Devaraj et al.,
273 2007; Frieman et al., 2009; Sadler and Williams, 2008). Interestingly, we identified OTUD4 as an
274 interacting partner of LotB. OTUD4 has been shown to deubiquitinate K63-linked chains of
275 myeoloid differentiation primary response 88 (MYD88) and to downregulate NF-kB-dependent
276 inflammation. While the recent study on LotB showed that there is no detectable inhibition of NF-
277 kB reporter expression(Ma et al., 2020), further studies are awaited to show the cross-talk between
278 LotB and host ubiquitination system.

279 *Legionella pneumophila* has been shown to possess multiple genes altering the host
280 ubiquitination system. However, little is known about functional cross-talk between ubiquitin
281 ligases and deubiquitinases. To understand the combinatorial effects of *Legionella* ubiquitin
282 ligases and deubiquitinases, we analyzed the interactome of LotB/LotC with host proteins in the
283 presence or absence of *Legionella* ligases (SidC and SdcA). We could see clear differences in the
284 number of enriched proteins in different combinations. Interestingly, we saw the clear difference
285 in the number of enriched proteins. A significant number of ribosomal proteins were enriched with
286 LotC in the background of SdcA, but not from SidC background, which has 71 % sequence
287 similarity to SdcA. This finding suggests distinct physiological roles of SdcA and SidC, and a
288 putative relationship between LotC and SdcA on regulating translation processes. Since LotC
289 processes different types of ubiquitin chains, and is mainly localized to the cytosol, a catalytically
290 dead version of LotC can be used as a standard tool for the identification of specific substrates of
291 other known *Legionella* ligases. It would be interesting to understand how all these ubiquitin

292 machineries synergistically work together and alter the host-ubiquitination system at different time
293 points of infection.
294
295 **MATERIAL AND METHODS**

296 **Protein expression and purification**

297 All proteins used in this study were expressed and purified as previously described (Bhogaraju et
298 al., 2016; Qiu et al., 2016). Lpg1621 (LotB), Lpg2529 (LotC), Lpg2411 and Lpg2907 were cloned
299 into either pParallelGST2 or pParallelHis2 vector (Sheffield et al., 1999). T7 express *E. coli*
300 competent cells (NEB) were transformed with plasmids and grown in LB medium to an OD_{600} of
301 0.6-0.8 at 37°C. Protein expression was induced by addition of 0.5 mM IPTG (isopropyl D-
302 thiogalactopyranoside) and the cells were further grown overnight at 18°C and harvested. The cell
303 pellet was resuspended in lysis buffer (50 mM Tris-HCl pH 7.5 and 150 mM NaCl, 2 mM DTT)
304 and lysed by sonication and centrifuged at 13,000 rpm to clarify the supernatant. The supernatant
305 of GST-tagged protein was incubated 1 hour with glutathione-*S*-sepharose pre-equilibrated with
306 washing buffer (50 mM Tris-HCl pH 7.5, 500 mM NaCl, 2 mM DTT) and non-specific proteins
307 were cleared with washing. GST-proteins were eluted with elution buffer (50 mM Tris-HCl pH
308 8.0, 50 mM NaCl, 2 mM DTT, 15 mM reduced glutathione) and buffer exchanged to storage buffer
309 (50 mM Tris-HCl pH 7.5, 150 mM NaCl, 1 mM DTT). For His-tagged proteins, the supernatant
310 was incubated with Ni-NTA pre-equilibrated with washing buffer (50 mM Tris-HCl, pH 7.5, 500
311 mM NaCl, 20 mM Imidazole) for 2 hours and eluted with elution buffer (50 mM Tris-HCl, pH 7.5,
312 500 mM NaCl, 300 mM Imidazole) and the buffer was exchanged to storage buffer. For $LotC_{14-}$
313 $_{310}$, instead of using the elution buffer, glutathione beads were incubated with sfGFP-TEV protease
314 (Wu et al., 2009) overnight at 4°C. Cleaved protein were buffer exchanged to IEX buffer A (20
315 mM Tris-HCl, pH 8.0, 20 mM NaCl, 1 mM DTT) and purified by anion-exchange chromatography
316 on HitrapQ (GE Healthcare) with gradient elution with IEX buffer B (20 mM Tris-HCl, pH 8.0, 1
317 M NaCl, 1 mM DTT) and fractions contacting samples were loaded onto size-exclusion column
318 (Superdex 75 16/60, GE Healthcare) pre-equilibrated with 50 mM Tris-HCl pH 7.5, 50 mM NaCl,
319 1 mM TCEP. Proteins were concentrated to 20 mg/ml and stored for crystallization.
320
321 **Di-Ub panel cleavage assay**

322 To activate DUBs, 3 µl of 5 µM of DUBs were mixed with 12 µl of activation buffer (25 mM Tris-
323 HCl pH 7.5, 150 mM NaCl, 10 mM DTT) and incubated 15 minutes at 25°C. For di-Ubiquitin
324 samples, 3 µl of di-ubiquitin chains (1 mg/ml) were mixed with 3 µl 10x reaction buffer (500 mM
325 Tris-HCl pH 7.5, 500 mM NaCl, 50 mM DTT) and 12 µl of ultra-pure water. To initiate the
326 reaction, the activated DUBs were mixed with di-Ubiquitin and samples were taken at the indicated
327 time points and the reactions were quenched by the addition of SDS-sample buffer. The samples
328 were further analyzed by SDS-PAGE and stained with silver-staining kit (Pierce Silver Staining
329 Kit, Thermo Fischer).
330
331 **Ubiquitin/NEDD8/SUMO-/ISG15/UFM activity-based probes assay**
332 DUBs were diluted (1.5 µM, final concentration) with activation buffer and incubated 10 minutes
333 at 25°C and the activity-based probes were diluted (50 µM, final concentration) in dilution buffer
334 (50 mM Tris-HCl 7.5, 150 mM NaCl). The total of 30 ul of reaction mixture was prepared by
335 mixing 20 µl of activated DUBs (1.5 µM), 3 µl of activity-based probes, 3 µl of reaction buffer
336 (500 mM Tris-HCl pH 7.5, 500 mM NaCl, 50 mM DTT) and 4 µl of ultra-pure water. Samples
337 were taken at the indicated time points and the reactions were quenched by the addition of SDS-
338 sample buffer. Samples were further analyzed by SDS-PAGE and stained with Coomassie staining
339 solution.
340
341 **Crystallization**
342 The concentrated $LotC_{14-310}$ were screened with sitting drop matrix screens in 96-well plate with
343 100 nl of protein and 100 nl of precipitant solution at 293K. Initial crystals appeared from solution
344 containing 25 % PEG3350, 100 mM Tris-HCl pH 8.5, 200 mM NaCl with 18.4 mg/ml protein
345 concentration. Diffraction-quality crystals were grown in optimized solution containing 19 % PEG
346 3350, 100 mM Tris-HCl pH 8.5, 150 mM NaCl with 24 mg/ml protein concentration.
347
348 **Data collection, processing and structure determination**
349 To obtain the phase, 0.4 µl of 10 mM K_2PtCl_4 was added to the drop containing crystals and
350 incubated for 18 hours. Heavy atom-soaked crystals were cryo-protected using mother liquor
351 solution supplemented with 15 % (v/v) glycerol. Diffraction data were collected on single frozen
352 crystal in a nitrogen stream at 100K at beamline PXI as Swiss Light Source, Villigen. Initial data

353 sets were processed using XDS (Kabsch, 2010), and initial-phases were determined by Autosol in
354 Phenix (Terwilliger et al., 2009). Structure refinement and manual model building were performed
355 with Coot and Phenix.Refine (Afonine et al., 2012; Emsley et al., 2010).
356
357 **Protein-protein docking**
358 We used the Rosetta protein-protein docking method (Gray et al., 2003) to identify low-energy
359 conformations of the complexes of ubiquitin with LotB and LotC, respectively. Given that the C-
360 terminus of ubiquitin should interact with the catalytic residue of the OTUs, we used the local
361 docking approach in which we placed the C-terminal end of ubiquitin (Gly76) near the catalytic
362 residues in both ligases (Cys29 and His270 for LotB and Cys16 and His296 for LotC). We then
363 started the docking by optimizing the rigid-body orientation and side-chain conformation sampling.
364 The program requires two protein structures as inputs, which were prepared by running the
365 refinement protocol before the docking step. We performed the local docking approach and
366 generated 100 independent structures for each complex. The complexes in this way were subject
367 to local refinement to remove remaining small clashes. The complexes were then clustered based
368 on the distance matrix of Cα atoms between the ligase and ubiquitin using the KMeans method.
369 The representatives of two major clusters in each case were selected based on the interface score
370 (I_sc), which represents the energy of the interactions across the interface of two proteins. These
371 representative complexes were used for MD simulations.
372
373 **Molecular dynamics simulations**
374 All-atom explicit solvent molecular dynamics (MD) simulations were performed for two docking
375 results for each ligase. The systems were built using the CHARMM-GUI webserver (Wu et al.,
376 2014). The systems were hydrated with 150 mM NaCl electrolyte. The all-atom CHARMM36m
377 force field was used for proteins, lipids and ions, and TIP3P was used for water molecules (Best
378 et al., 2012). The MD trajectories were analyzed with Visual Molecular Dynamics (VMD)
379 (Humphrey et al., 1996). The MD simulations were performed using GROMACS 2019 (Abraham
380 et al., 2015). The starting system was minimized for 5,000 steps with the steepest descent energy
381 minimization and equilibrated for 6.5 ns of MD simulation first in the NVT ensemble (1.5 ns) and
382 then in the NPT (5 ns) ensemble, in which all non-hydrogen atoms of the protein were restrained
383 to the fixed reference positions with progressively reduced force constants, starting at 1000

384 kJ·mol^{-1}·nm^2. Afterwards, the production runs were carried out in the NPT ensemble for 600 ns
385 for each setup. To keep the C-terminusof ubiquitin in the catalytic site, 7-Å wall restraints were
386 placed on the distance between Cα of $G76_{UB}$ and Cys29/His270 in LotB and between Cα of $G76_{UB}$
387 and Cys16/His296 in LotC. Periodic boundary conditions were used. Particle mesh Ewald (Darden
388 et al., 1993) with cubic interpolation and 0.12 nm grid spacing for Fast Fourier Transform was
389 used to treat long-range electrostatic interactions. The time step was 2 fs. The LINCS algorithm
390 (Hess et al., 1997) was used to fix all bond lengths. Constant temperature (310 K) was set with a
391 Nosé-Hoover thermostat (Hoover, 1985), with a coupling constant of 1.0 ps. An isotropic
392 Parrinello-Rahman barostat (Parrinello and Rahman, 1981) with a coupling constant of 5.0 ps was
393 used to maintain a pressure of 1 bar.
394
395 **Identification of novel substrates of LotB and LotC**
396 For interactome analysis, HEK 293 cells were transfected with FLAG-LotB WT/C29A or FLAG-
397 LotC WT/C24A. To identify the substrates modified by *Legionella* derived E3 ligases, GFP-SidC
398 or GFP-SdcA were co-transfected with FLAG-LotB WT/C29A or FLAF-LotC WT/C24A.
399 Cells were lysed in ice cold lysis buffer (50mM Tris-Cl, p.H 7.5; 150mM NaCl; 1% Triton x-100)
400 and equal amount of lysates were incubated with FLAG-M2 beads in IP buffer (Lysis buffer
401 without detergent). After incubation, IPs were washed with wash buffer (50mM Tris-Cl, pH7.5;
402 400mM NaCl; 0.5mM EDTA) and the interacting proteins were eluted with 8M urea solution.
403 After the reduction and alkylation with TCEP and Chloroacetamide, the samples were digested
404 with 0.5ug Trypsin (Promega) at 37°C overnight after diluting the urea < 2M. Digests were
405 acidified using trifluoroaceticacid (TFA) to a pH of 2-3, and the peptides were enriched using C18
406 stage tips (Rappsilber et al., 2003). To get quantitative information, peptides were either labelled
407 with TMT 10 plex reagent (Thermo fisher) or analyzed label-free. The peptides were separated on
408 an in-house made C18 column (20 cm length, 75 µm inner diameter, 1.9 µm particle size) by an
409 easy n-LC 1200 (ThermoFisher) and directly injected in a QExactive-HF or in case of TMT
410 samples into a Fusion Lumos mass-spectrometer (ThermoFisher) and analyzed in data-dependent
411 mode. Data analysis was done using Maxquant 1.65 (Cox and Mann, 2008). Fragment spectra
412 were searched against *Homo sapiens* SwissProt database (TaxID:9606, version 2018). Label-free
413 quantification was done with MaxLFQ (Cox et al., 2014) method with activated match between
414 runs. TMT-labelled samples were analysed by using TMT 10 Plex option within the software.

415 Statistically significant changes between samples were determined using a Two-sample t-test with
416 a permutation-based FDR of 5% on log2 transformed values in Perseus (Tyanova et al., 2016).
417
418 **Confocal imaging and image analysis**
419 U2OS cells were transfected with FLAG-LotB or FLAG-LotC by GeneJuice transfection reagent
420 (Merck) for 24 h and fixed by 4% paraformaldehyde for 20 min. After fixation, cells were
421 permeabilized and blocked by 0.1% saponin and 1% BSA in PBS for 1 h at room temperature.
422 Cells were incubated with anti-Flag antibody (Sigma and Cell Signaling), with either anti-calnexin
423 antibody (Abcam), anti-TOMM20 antibody (Abcam), or anti-GM130 (BD Transduction
424 Laboratories) at 4 °C overnight. Alexa Fluor 488 and Alexa Fluor 546 (Invitrogen) secondary
425 antibody were incubated for 1 h at room temperature. Images were acquired by the Zeiss LSM780
426 microscope system with 63× 1.4 NA oil immersion objective and further analyzed by Zeiss Zen
427 microscope software.
428
429 **ACKNOWLEDGEMENTS:**
430

431 We thank Yuxin-Mao for providing SidC and SdcA clones and Stefan Knapp for the advice in
432 structure determination and sharing synchrotron time. The authors also thank staff at SLS for their
433 support during crystallographic X-ray diffraction test and data collection. The data collection at
434 SLS has been supported by the funding from the European Union's Horizon 2020 research and
435 innovation program under grant agreement number 730872, project CALIPSOplus. This project
436 was supported by the European Research Council (ERC) under the European Union's Horizon
437 2020 research and innovation program (ID, grant agreement No 742720), the LOEWE program
438 DynaMem of the State of Hesse (Germany, Project-ID III L6-519/03/03.001 – (0006)), and
439 Deutsche Forschungsgemeinschaft (DFG, German Research Foundation (Project-ID 259130777 –
440 SFB1177; Leibniz-Program to ID; CEF-MC - EXC115/2; SFB 902), the Max Planck Society and
441 NWO-VIDI grant and Off-rad grand for G.H.
442

COMPETING INTERSTES: The authors declare no competing interests.

445 **Figure Legends and Tables:**

446 **Table1. TOP 5 candidates for putative DUBs from Legionella effector proteins**

Legionella Proteins		Target Proteins				
Name	Aligned Region	Name	Aligned Region	Probability (%)	Identities (%)	PDB ID_Chain
Lpg1621	195-274	Viral OTU (CC hemorrhagic fever virus)	69-157	92.59	16	3PHU_B
	195-274	Human OTUD2	63-140	92.52	17	4BOQ_A
	195-279	Human OTUD3	59-142	92.40	13	4BOU_A
	193-278	Human OTUD5	100-183	91.18	21	3PFY_A
	192-279	Viral OTU (Farallon virus)	88-183	91.08	16	6DX5_B
Lpg2529	1-310	Viral OTU (Erve virus)	17-157	96.24	18	5JZE_A
	7-310	Viral OTU (Dera Ghazi Khan orthonairovirus)	25-156	96.15	18	6DX2_B
	20-310	Human Otubain1	50-234	96.02	13	2ZFY_A
	20-310	Human Otubain2	50-233	95.84	13	4FJV_C
	7-310	Viral OTU (Taggert virus)	23-156	95.71	13	6DX3_D
Lpg2411	110-216	Yeast UCH8	152-259	37.94	11	3MHS_A
	183-272	EntA-im (Enterococcus faecium)	7-89	37.06	15	2BL8_B
	33-94	Uncharacterized protein (Corynebacterium diphtheriae)	7-72	36.65	21	3KDQ_D
	120-212	PG0816 (Porphyromonas gingivalis)	53-139	35.31	16	2APL_A
	104-114	PSII reaction center protein K (Cyanidium caldarium)	2-12	32.96	36	4YUU_X2
Lpg2907	117-384	AvrA (Salmonella typhimurium)	59-299	100	11	6BE0_A
	158-398	PopP2 (Arabidopsis thaliana)	99-339	99.93	13	5W3X_C
	115-390	HopZ1a (Pseudomonas syringae)	54-342	99.88	10	5KLP_C
	118-275	XopD (Xanthomonas campestris)	1-148	95.53	11	2OIX_A
	95-276	Human SENP1	2-177	95.21	16	2G4D_A

447 Values are obtained from HHpred server (MPI Bioinformatics Toolkit)

448

449 **Figure 1. Identification of novel deubiqutinases in *Legionella pneumophila.***

450 **(a)** Graphical illustration of identification of novel deubiquitinases of Legionella pneumophila Lpg

451 Genes. **(b)** Predicted deubiquitinase domain of four putative *Legionella* deubiquitinases. **(c, e)**

452 Time-course Di-ubiquitin panel cleavage assay with Lpg1621 (LotB) and Lpg2529 (LotC),

453 respectively. **(d, f)** Linkage specificity diagram of Lpg1621 (LotB) and Lpg2529 (LotC).

454 Percentage of cleaved ubiquitin species at 90 mins were plotted.

455

456 **Figure 2. Biochemical properties of LotB and LotC**

457 **(a)** Predicted catalytic residues on LotB and LotC. **(b, c)** Di-Ub cleavage activity assay with wild-
458 type and catalytic mutants of LotB and LotC, respectively. **(d, e)** Activity based probes (ABPs)
459 test on LotB and LotC. Propargyl-Ub-ABP (Prg-ABP) and vinylmethylester-ubiquitin-ABP
460 (VME-ABP) were incubated as indicated time-points with LotB and LotC and analyzed on SDS-
461 PAGE with Coomassie staining. **(f, g)** Propargyl ubiquitin or ubiquitin-like modifiers reactivity
462 test on LotB and LotC. Prg-ABPs are incubated with LotB and LotC with indicated time points.

463

464 **Figure 3. Structural comparison of *Legionella* OTU-DUBs with other OTU-family**

465 **(a, b)** Minimal domain boundaries of catalytically active LotB and LotC. Different constructs were
466 cloned based on the predicted OTU-domains and their activity, and were tested with di-Ub_2 panel
467 **(c, d)** Structural comparison of LotB and LotC with their closest homologues. CCHF- (PDB:
468 3PHU), Farallon- (PDB: 6DX5), OTUD2 (PDB: 4BOQ), OTUD3 (PDB: 4BOU), Taggert- (PDB:
469 6DX3), DGK nairo- (PDB: 6DX2), Otubain1 (PDB: 2ZFY), Otubain2 (PDB: 4FJV). **(e)** Sequence
470 alignment of LotB and LotC with their closest homologues. Catalytic cysteine and histidine are
471 highlighted in red and conserved residues are highlighted in yellow.

472

473 **Figure 4. Ubiquitin binding sites on LotB and LotC**

474 **(a, b)** Molecular docking and simulations of monoubiquitin to LotB and LotC, respectively. Shown
475 are representative snapshots of the MD simulations. Catalytic cysteine and key residues for the
476 interaction between ubiquitin and LotB or LorC are depicted as sticks. **(c, d)** Key residues
477 mediating interactions of ubiquitin with LotB and LotC, respectively. Residues are highlighted in
478 the structure (left). Side-chain center-of-mass distances are shown as a function of the simulation
479 time (right). **(e, f)** Di-ubiquitin cleavage assay for mutants of LotB and LotC. The catalytic activity
480 of LotB or LotC wild-type and its mutants was tested with K63- or K48- linked Ub2, respectively.
481

482 **Figure 5. Physiological roles of LotB and LotC**

483 **(a, c)** Proteomic analysis of interacting partners of LotB and LotC, respectively. Catalytically
484 inactive FLAG-LotB (C29A) and FLAG-LotC (C24A) were transfected and immunoprecipitated.
485 Co-precipitated interacting proteins were analyzed by mass spectrometry. **(b, d)** Cellular
486 localization of LotB and LotC. FLAG-tagged LotB and LotC were ectopically expressed in U2OS
487 cells and immunostained with cellular organelle markers (ER; Calnexin, Mitochondria: TOMM20,
488 Golgi: GM130). **(e, f)** List of significantly enriched proteins from LotB and LotC with or without
489 *Legionella* ligases (SdcA or SidC) as indicated.

490

491 **REFERENCES:**

492 Abdul Rehman SA, Kristariyanto YA, Choi S-Y, Nkosi PJ, Weidlich S, Labib K, Hofmann K,
493 Kulathu Y. 2016. MINDY-1 Is a Member of an Evolutionarily Conserved and Structurally
494 Distinct New Family of Deubiquitinating Enzymes. *Mol Cell* **63**:146–155.
495 doi:10.1016/j.molcel.2016.05.009

496 Abraham MJ, Murtola T, Schulz R, Páll S, Smith JC, Hess B, Lindahl E. 2015. GROMACS:
497 High performance molecular simulations through multi-level parallelism from laptops to
498 supercomputers. *SoftwareX* **1**–**2**:19–25. doi:10.1016/j.softx.2015.06.001

499 Afonine P V., Grosse-Kunstleve RW, Echols N, Headd JJ, Moriarty NW, Mustyakimov M,
500 Terwilliger TC, Urzhumtsev A, Zwart PH, Adams PD. 2012. Towards automated
501 crystallographic structure refinement with phenix.refine. *Acta Crystallogr Sect D Biol*
502 *Crystallogr* **68**:352–367. doi:10.1107/S0907444912001308

503 Akutsu M, Ye Y, Virdee S, Chin JW, Komander D. 2011. Molecular basis for ubiquitin and
504 ISG15 cross-reactivity in viral ovarian tumor domains. *Proc Natl Acad Sci* **108**:2228–2233.
505 doi:10.1073/pnas.1015287108

506 Best RB, Zhu X, Shim J, Lopes PEM, Mittal J, Feig M, MacKerell AD. 2012. Optimization of
507 the Additive CHARMM All-Atom Protein Force Field Targeting Improved Sampling of the
508 Backbone ϕ, ψ and Side-Chain χ 1 and χ 2 Dihedral Angles. *J Chem Theory Comput*
509 **8**:3257–3273. doi:10.1021/ct300400x

510 Bhogaraju S, Bonn F, Mukherjee R, Adams M, Pfleiderer MM, Galej WP, Matkovic V, Lopez-
511 Mosqueda J, Kalayil S, Shin D, Dikic I. 2019. Inhibition of bacterial ubiquitin ligases by
512 SidJ–calmodulin catalysed glutamylation. *Nature* **572**:382–386. doi:10.1038/s41586-019-
513 1440-8

514 Bhogaraju S, Kalayil S, Liu Y, Bonn F, Colby T, Matic I, Dikic I. 2016. Phosphoribosylation of
515 Ubiquitin Promotes Serine Ubiquitination and Impairs Conventional Ubiquitination. *Cell*
516 **167**:1636-1649.e13. doi:10.1016/j.cell.2016.11.019

517 Black MH, Osinski A, Gradowski M, Servage KA, Pawłowski K, Tomchick DR, Tagliabracci
518 VS. 2019. Bacterial pseudokinase catalyzes protein polyglutamylation to inhibit the SidE-
519 family ubiquitin ligases. *Science (80-)* **364**:787–792. doi:10.1126/science.aaw7446

520 Borodovsky A, Ovaa H, Kolli N, Gan-Erdene T, Wilkinson KD, Ploegh HL, Kessler BM. 2002.
521 Chemistry-Based Functional Proteomics Reveals Novel Members of the Deubiquitinating

522 Enzyme Family. *Chem Biol* **9**:1149–1159. doi:10.1016/S1074-5521(02)00248-X
523 Bremm A, Freund SM V, Komander D. 2010. Lys11-linked ubiquitin chains adopt compact
524 conformations and are preferentially hydrolyzed by the deubiquitinase Cezanne. *Nat Struct*
525 *Mol Biol* **17**:939–947. doi:10.1038/nsmb.1873
526 Burstein D, Amaro F, Zusman T, Lifshitz Z, Cohen O, Gilbert JA, Pupko T, Shuman HA, Segal
527 G. 2016. Genomic analysis of 38 Legionella species identifies large and diverse effector
528 repertoires. *Nat Genet* **48**:167–175. doi:10.1038/ng.3481
529 Capodagli GC, Deaton MK, Baker EA, Lumpkin RJ, Pegan SD. 2013. Diversity of Ubiquitin and
530 ISG15 Specificity among Nairoviruses' Viral Ovarian Tumor Domain Proteases. *J Virol*
531 **87**:3815–3827. doi:10.1128/JVI.03252-12
532 Clague MJ, Urbé S, Komander D. 2019. Breaking the chains: deubiquitylating enzyme
533 specificity begets function. *Nat Rev Mol Cell Biol* **20**:338–352. doi:10.1038/s41580-019-
534 0099-1
535 Cox J, Hein MY, Luber CA, Paron I, Nagaraj N, Mann M. 2014. Accurate Proteome-wide Label-
536 free Quantification by Delayed Normalization and Maximal Peptide Ratio Extraction,
537 Termed MaxLFQ. *Mol Cell Proteomics* **13**:2513–2526. doi:10.1074/mcp.M113.031591
538 Cox J, Mann M. 2008. MaxQuant enables high peptide identification rates, individualized p.p.b.-
539 range mass accuracies and proteome-wide protein quantification. *Nat Biotechnol* **26**:1367–
540 1372. doi:10.1038/nbt.1511
541 Darden T, York D, Pedersen L. 1993. Particle mesh Ewald: An N ·log(N) method for Ewald
542 sums in large systems. *J Chem Phys* **98**:10089–10092. doi:10.1063/1.464397
543 Davis ME, Gack MU. 2015. Ubiquitination in the antiviral immune response. *Virology* **479**–
544 **480**:52–65. doi:10.1016/j.virol.2015.02.033
545 Devaraj SG, Wang N, Chen Zhongbin, Chen Zihong, Tseng M, Barretto N, Lin R, Peters CJ,
546 Tseng C-TK, Baker SC, Li K. 2007. Regulation of IRF-3-dependent Innate Immunity by the
547 Papain-like Protease Domain of the Severe Acute Respiratory Syndrome Coronavirus. *J*
548 *Biol Chem* **282**:32208–32221. doi:10.1074/jbc.M704870200
549 Diao J, Zhang Y, Huibregtse JM, Zhou D, Chen J. 2008. Crystal structure of SopA, a Salmonella
550 effector protein mimicking a eukaryotic ubiquitin ligase. *Nat Struct Mol Biol* **15**:65–70.
551 doi:10.1038/nsmb1346
552 Dikic I. 2017. Proteasomal and Autophagic Degradation Systems. *Annu Rev Biochem* **86**:193–

553 224. doi:10.1146/annurev-biochem-061516-044908
554 Edelmann MJ, Iphöfer A, Akutsu M, Altun M, di Gleria K, Kramer HB, Fiebiger E, Dhe-
555 Paganon S, Kessler BM. 2009. Structural basis and specificity of human otubain 1-mediated
556 deubiquitination. *Biochem J* **418**:379–390. doi:10.1042/BJ20081318
557 Ekkebus R, van Kasteren SI, Kulathu Y, Scholten A, Berlin I, Geurink PP, de Jong A, Goerdayal
558 S, Neefjes J, Heck AJR, Komander D, Ovaa H. 2013. On Terminal Alkynes That Can React
559 with Active-Site Cysteine Nucleophiles in Proteases. *J Am Chem Soc* **135**:2867–2870.
560 doi:10.1021/ja309802n
561 El Oualid F, Merkx R, Ekkebus R, Hameed DS, Smit JJ, de Jong A, Hilkmann H, Sixma TK,
562 Ovaa H. 2010. Chemical Synthesis of Ubiquitin, Ubiquitin-Based Probes, and Diubiquitin.
563 *Angew Chemie Int Ed* **49**:10149–10153. doi:10.1002/anie.201005995
564 Emsley P, Lohkamp B, Scott WG, Cowtan K. 2010. Features and development of Coot. *Acta*
565 *Crystallogr Sect D Biol Crystallogr* **66**:486–501. doi:10.1107/S0907444910007493
566 Ensminger AW, Isberg RR. 2010. E3 Ubiquitin Ligase Activity and Targeting of BAT3 by
567 Multiple Legionella pneumophila Translocated Substrates. *Infect Immun* **78**:3905–3919.
568 doi:10.1128/IAI.00344-10
569 Fiskin E, Bhogaraju S, Herhaus L, Kalayil S, Hahn M, Dikic I. 2017. Structural basis for the
570 recognition and degradation of host TRIM proteins by Salmonella effector SopA. *Nat*
571 *Commun* **8**:14004. doi:10.1038/ncomms14004
572 Flierman D, van der Heden van Noort GJ, Ekkebus R, Geurink PP, Mevissen TET, Hospenthal
573 MK, Komander D, Ovaa H. 2016. Non-hydrolyzable Diubiquitin Probes Reveal Linkage-
574 Specific Reactivity of Deubiquitylating Enzymes Mediated by S2 Pockets. *Cell Chem Biol*
575 **23**:472–482. doi:10.1016/j.chembiol.2016.03.009
576 Frieman M, Ratia K, Johnston RE, Mesecar AD, Baric RS. 2009. Severe Acute Respiratory
577 Syndrome Coronavirus Papain-Like Protease Ubiquitin-Like Domain and Catalytic Domain
578 Regulate Antagonism of IRF3 and NF- B Signaling. *J Virol* **83**:6689–6705.
579 doi:10.1128/JVI.02220-08
580 Furtado AR, Essid M, Perrinet S, Balañá ME, Yoder N, Dehoux P, Subtil A. 2013. The
581 chlamydial OTU domain-containing protein Chla OTU is an early type III secretion effector
582 targeting ubiquitin and NDP52. *Cell Microbiol* **15**:2064–2079. doi:10.1111/cmi.12171
583 Gray JJ, Moughon SE, Kortemme T, Schueler-Furman O, Misura KMS, Morozov A V., Baker

584 D. 2003. Protein-protein docking predictions for the CAPRI experiment. *Proteins Struct*
585 *Funct Genet* **52**:118–122. doi:10.1002/prot.10384
586 Haahr P, Borgermann N, Guo X, Typas D, Achuthankutty D, Hoffmann S, Shearer R, Sixma
587 TK, Mailand N. 2018. ZUFSP Deubiquitylates K63-Linked Polyubiquitin Chains to
588 Promote Genome Stability. *Mol Cell* **70**:165-174.e6. doi:10.1016/j.molcel.2018.02.024
589 Hermanns T, Hofmann K. 2019. Bacterial DUBs: deubiquitination beyond the seven classes.
590 *Biochem Soc Trans* **47**:1857–1866. doi:10.1042/BST20190526
591 Hermanns T, Pichlo C, Woiwode I, Klopffleisch K, Witting KF, Ovaa H, Baumann U, Hofmann
592 K. 2018. A family of unconventional deubiquitinases with modular chain specificity
593 determinants. *Nat Commun* **9**:799. doi:10.1038/s41467-018-03148-5
594 Hess B, Bekker H, Berendsen HJC, Fraaije JGEM. 1997. LINCS: A linear constraint solver for
595 molecular simulations. *J Comput Chem* **18**:1463–1472. doi:10.1002/(SICI)1096-
596 987X(199709)18:12<1463::AID-JCC4>3.0.CO;2-H
597 Hewings DS, Heideker J, Ma TP, AhYoung AP, El Oualid F, Amore A, Costakes GT,
598 Kirchhofer D, Brasher B, Pillow T, Popovych N, Maurer T, Schwerdtfeger C, Forrest WF,
599 Yu K, Flygare J, Bogyo M, Wertz IE. 2018. Reactive-site-centric chemoproteomics
600 identifies a distinct class of deubiquitinase enzymes. *Nat Commun* **9**:1162.
601 doi:10.1038/s41467-018-03511-6
602 Hoover WG. 1985. Canonical dynamics: Equilibrium phase-space distributions. *Phys Rev A*
603 **31**:1695–1697. doi:10.1103/PhysRevA.31.1695
604 Hsu F, Luo X, Qiu J, Teng Y-B, Jin J, Smolka MB, Luo Z-Q, Mao Y. 2014. The Legionella
605 effector SidC defines a unique family of ubiquitin ligases important for bacterial
606 phagosomal remodeling. *Proc Natl Acad Sci* **111**:10538–10543.
607 doi:10.1073/pnas.1402605111
608 Humphrey W, Dalke A, Schulten K. 1996. VMD: Visual molecular dynamics. *J Mol Graph*
609 **14**:33–38. doi:10.1016/0263-7855(96)00018-5
610 James TW, Frias-Staheli N, Bacik J-P, Levingston Macleod JM, Khajehpour M, Garcia-Sastre A,
611 Mark BL. 2011. Structural basis for the removal of ubiquitin and interferon-stimulated gene
612 15 by a viral ovarian tumor domain-containing protease. *Proc Natl Acad Sci* **108**:2222–
613 2227. doi:10.1073/pnas.1013388108
614 Kabsch W. 2010. XDS. *Acta Crystallogr Sect D Biol Crystallogr* **66**:125–132.

615 doi:10.1107/S0907444909047337
616 Kalayil S, Bhogaraju S, Bonn F, Shin D, Liu Y, Gan N, Basquin J, Grumati P, Luo Z-Q, Dikic I.
617 2018. Insights into catalysis and function of phosphoribosyl-linked serine ubiquitination.
618 *Nature* **557**:734–738. doi:10.1038/s41586-018-0145-8
619 Keusekotten K, Elliott PR, Glockner L, Fiil BK, Damgaard RB, Kulathu Y, Wauer T,
620 Hospenthal MK, Gyrd-Hansen M, Krappmann D, Hofmann K, Komander D. 2013.
621 OTULIN Antagonizes LUBAC Signaling by Specifically Hydrolyzing Met1-Linked
622 Polyubiquitin. *Cell* **153**:1312–1326. doi:10.1016/j.cell.2013.05.014
623 Kubori T, Hyakutake A, Nagai H. 2008. Legionella translocates an E3 ubiquitin ligase that has
624 multiple U-boxes with distinct functions. *Mol Microbiol* **67**:1307–1319. doi:10.1111/j.1365-
625 2958.2008.06124.x
626 Kubori T, Kitao T, Ando H, Nagai H. 2018. LotA, a Legionella deubiquitinase, has dual catalytic
627 activity and contributes to intracellular growth. *Cell Microbiol* **20**:e12840.
628 doi:10.1111/cmi.12840
629 Kwasna D, Abdul Rehman SA, Natarajan J, Matthews S, Madden R, De Cesare V, Weidlich S,
630 Virdee S, Ahel I, Gibbs-Seymour I, Kulathu Y. 2018. Discovery and Characterization of
631 ZUFSP/ZUP1, a Distinct Deubiquitinase Class Important for Genome Stability. *Mol Cell*
632 **70**:150-164.e6. doi:10.1016/j.molcel.2018.02.023
633 Lin DY -w., Diao J, Chen J. 2012. Crystal structures of two bacterial HECT-like E3 ligases in
634 complex with a human E2 reveal atomic details of pathogen-host interactions. *Proc Natl*
635 *Acad Sci* **109**:1925–1930. doi:10.1073/pnas.1115025109
636 Lombardi C, Ayach M, Beaurepaire L, Chenon M, Andreani J, Guerois R, Jupin I, Bressanelli S.
637 2013. A Compact Viral Processing Proteinase/Ubiquitin Hydrolase from the OTU Family.
638 *PLoS Pathog* **9**:e1003560. doi:10.1371/journal.ppat.1003560
639 Ma K, Zhen X, Zhou B, Gan N, Cao Y, Fan C, Ouyang S, Luo Z-Q, Qiu J. 2020. The bacterial
640 deubiquitinase Ceg23 regulates the association of Lys-63–linked polyubiquitin molecules
641 on the Legionella phagosome. *J Biol Chem* **295**:1646–1657. doi:10.1074/jbc.RA119.011758
642 Mevissen TET, Hospenthal MK, Geurink PP, Elliott PR, Akutsu M, Arnaudo N, Ekkebus R,
643 Kulathu Y, Wauer T, El Oualid F, Freund SMV, Ovaa H, Komander D. 2013. OTU
644 Deubiquitinases Reveal Mechanisms of Linkage Specificity and Enable Ubiquitin Chain
645 Restriction Analysis. *Cell* **154**:169–184. doi:10.1016/j.cell.2013.05.046

646 Mevissen TET, Komander D. 2017. Mechanisms of Deubiquitinase Specificity and Regulation.
647 *Annu Rev Biochem* **86**:159–192. doi:10.1146/annurev-biochem-061516-044916
648 Mevissen TET, Kulathu Y, Mulder MPC, Geurink PP, Maslen SL, Gersch M, Elliott PR, Burke
649 JE, van Tol BDM, Akutsu M, El Oualid F, Kawasaki M, Freund SMV, Ovaa H, Komander
650 D. 2016. Molecular basis of Lys11-polyubiquitin specificity in the deubiquitinase Cezanne.
651 *Nature* **538**:402–405. doi:10.1038/nature19836
652 Mulder MPC, El Oualid F, ter Beek J, Ovaa H. 2014. A Native Chemical Ligation Handle that
653 Enables the Synthesis of Advanced Activity-Based Probes: Diubiquitin as a Case Study.
654 *ChemBioChem* **15**:946–949. doi:10.1002/cbic.201402012
655 Parrinello M, Rahman A. 1981. Polymorphic transitions in single crystals: A new molecular
656 dynamics method. *J Appl Phys* **52**:7182–7190. doi:10.1063/1.328693
657 Pohl C, Dikic I. 2019. Cellular quality control by the ubiquitin-proteasome system and
658 autophagy. *Science (80-)* **366**:818–822. doi:10.1126/science.aax3769
659 Pruneda JN, Durkin CH, Geurink PP, Ovaa H, Santhanam B, Holden DW, Komander D. 2016.
660 The Molecular Basis for Ubiquitin and Ubiquitin-like Specificities in Bacterial Effector
661 Proteases. *Mol Cell* **63**:261–276. doi:10.1016/j.molcel.2016.06.015
662 Qiu J, Sheedlo MJ, Yu K, Tan Y, Nakayasu ES, Das C, Liu X, Luo Z-Q. 2016. Ubiquitination
663 independent of E1 and E2 enzymes by bacterial effectors. *Nature* **533**:120–124.
664 doi:10.1038/nature17657
665 Quaile AT, Urbanus ML, Stogios PJ, Nocek B, Skarina T, Ensminger AW, Savchenko A. 2015.
666 Molecular Characterization of LubX: Functional Divergence of the U-Box Fold by
667 Legionella pneumophila. *Structure* **23**:1459–1469. doi:10.1016/j.str.2015.05.020
668 Rappsilber J, Ishihama Y, Mann M. 2003. Stop and Go Extraction Tips for Matrix-Assisted
669 Laser Desorption/Ionization, Nanoelectrospray, and LC/MS Sample Pretreatment in
670 Proteomics. *Anal Chem* **75**:663–670. doi:10.1021/ac026117i
671 Rawlings ND, Barrett AJ, Thomas PD, Huang X, Bateman A, Finn RD. 2018. The MEROPS
672 database of proteolytic enzymes, their substrates and inhibitors in 2017 and a comparison
673 with peptidases in the PANTHER database. *Nucleic Acids Res* **46**:D624–D632.
674 doi:10.1093/nar/gkx1134
675 Sadler AJ, Williams BRG. 2008. Interferon-inducible antiviral effectors. *Nat Rev Immunol*
676 **8**:559–568. doi:10.1038/nri2314

677 Sheffield P, Garrard S, Derewenda Z. 1999. Overcoming expression and purification problems of
678 RhoGDI using a family of "parallel" expression vectors. *Protein Expr Purif* **15**:34–9.
679 doi:10.1006/prep.1998.1003
680 Shin D, Mukherjee R, Liu Yaobin, Gonzalez A, Bonn F, Liu Yan, Rogov V V., Heinz M, Stolz
681 A, Hummer G, Dötsch V, Luo Z-Q, Bhogaraju S, Dikic I. 2020. Regulation of
682 Phosphoribosyl-Linked Serine Ubiquitination by Deubiquitinases DupA and DupB. *Mol*
683 *Cell* **77**:164-179.e6. doi:10.1016/j.molcel.2019.10.019
684 Sommer S, Weikart ND, Linne U, Mootz HD. 2013. Covalent inhibition of SUMO and
685 ubiquitin-specific cysteine proteases by an in situ thiol–alkyne addition. *Bioorg Med Chem*
686 **21**:2511–2517. doi:10.1016/j.bmc.2013.02.039
687 Terwilliger TC, Adams PD, Read RJ, McCoy AJ, Moriarty NW, Grosse-Kunstleve RW, Afonine
688 P V., Zwart PH, Hung L-W. 2009. Decision-making in structure solution using Bayesian
689 estimates of map quality: the PHENIX AutoSol wizard. *Acta Crystallogr Sect D Biol*
690 *Crystallogr* **65**:582–601. doi:10.1107/S0907444909012098
691 Tyanova S, Temu T, Sinitcyn P, Carlson A, Hein MY, Geiger T, Mann M, Cox J. 2016. The
692 Perseus computational platform for comprehensive analysis of (prote)omics data. *Nat*
693 *Methods* **13**:731–740. doi:10.1038/nmeth.3901
694 van Kasteren PB, Bailey-Elkin BA, James TW, Ninaber DK, Beugeling C, Khajehpour M,
695 Snijder EJ, Mark BL, Kikkert M. 2013. Deubiquitinase function of arterivirus papain-like
696 protease 2 suppresses the innate immune response in infected host cells. *Proc Natl Acad Sci*
697 **110**:E838–E847. doi:10.1073/pnas.1218464110
698 Wang T, Yin L, Cooper EM, Lai M-Y, Dickey S, Pickart CM, Fushman D, Wilkinson KD,
699 Cohen RE, Wolberger C. 2009. Evidence for Bidentate Substrate Binding as the Basis for
700 the K48 Linkage Specificity of Otubain 1. *J Mol Biol* **386**:1011–1023.
701 doi:10.1016/j.jmb.2008.12.085
702 Wasilko DJ, Huang Q, Mao Y. 2018. Insights into the ubiquitin transfer cascade catalyzed by the
703 Legionella effector SidC. *Elife* **7**:e36154. doi:10.7554/eLife.36154
704 Wu EL, Cheng X, Jo S, Rui H, Song KC, Dávila-Contreras EM, Qi Y, Lee J, Monje-Galvan V,
705 Venable RM, Klauda JB, Im W. 2014. CHARMM-GUI Membrane Builder toward realistic
706 biological membrane simulations. *J Comput Chem* **35**:1997–2004. doi:10.1002/jcc.23702
707 Wu X, Wu D, Lu Z, Chen W, Hu X, Ding Y. 2009. A Novel Method for High-Level Production

708 of TEV Protease by Superfolder GFP Tag. *J Biomed Biotechnol* **2009**:1–8.
709 doi:10.1155/2009/591923
710 Yau R, Rape M. 2016. The increasing complexity of the ubiquitin code. *Nat Cell Biol* **18**:579–
711 586. doi:10.1038/ncb3358
712 Zimmermann L, Stephens A, Nam S-Z, Rau D, Kübler J, Lozajic M, Gabler F, Söding J, Lupas
713 AN, Alva V. 2018. A Completely Reimplemented MPI Bioinformatics Toolkit with a New
714 HHpred Server at its Core. *J Mol Biol* **430**:2237–2243. doi:10.1016/j.jmb.2017.12.007
715
716

Figure 1

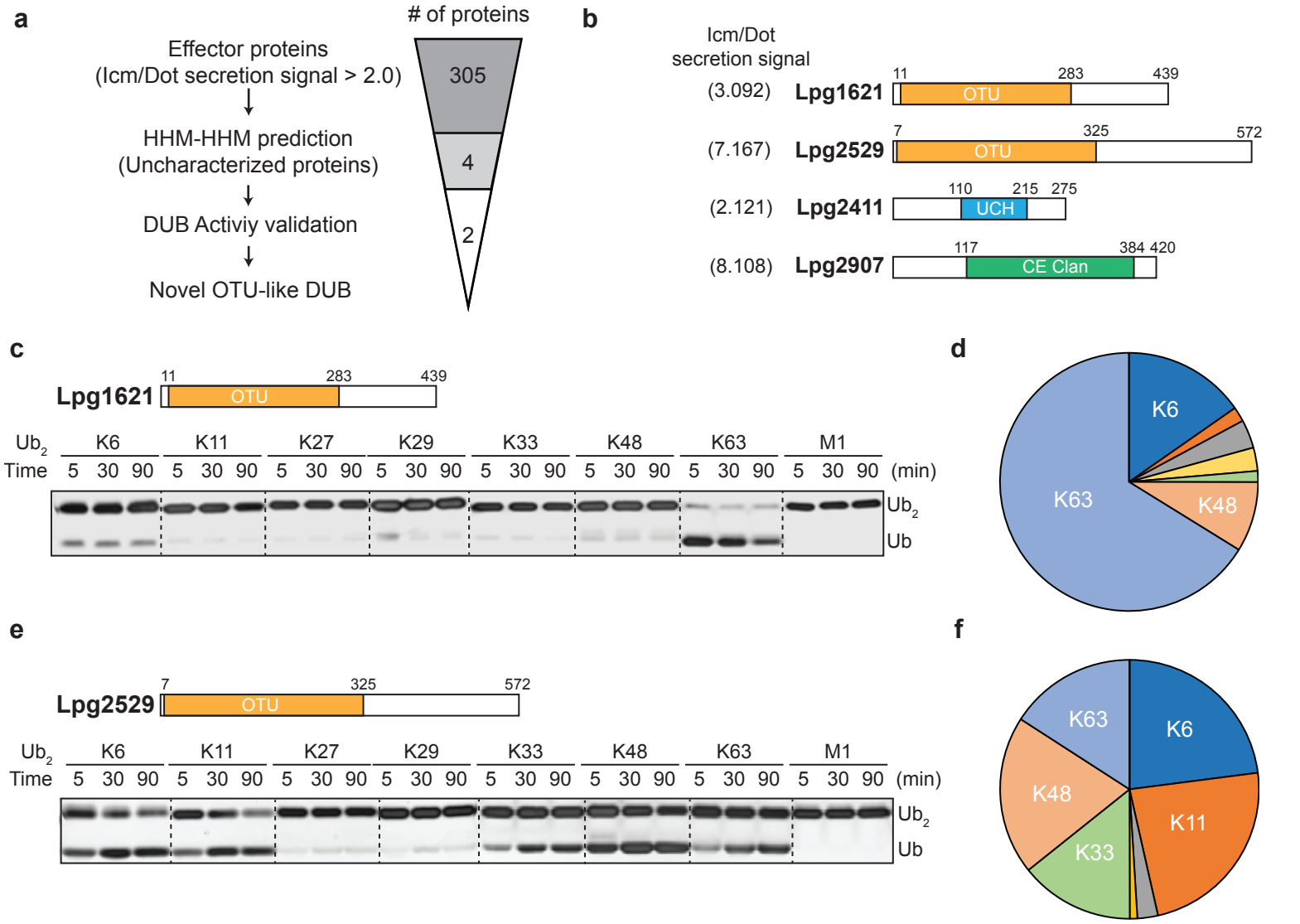
a
# of proteins
Effector proteins
(Icm/Dot secretion signal > 2.0)
305
HHM-HHM prediction
(Uncharacterized proteins)
4
DUB Activiy validation
2
Novel OTU-like DUB
b
Icm/Dot
secretion signal
(3.092) Lpg1621 11 283 439 OTU
(7.167) Lpg2529 7 325 572 OTU
(2.121) Lpg2411 110 215 275 UCH
(8.108) Lpg2907 117 384 420 CE Clan
c
Lpg1621 11 283 439 OTU
Ub2 K6 K11 K27 K29 K33 K48 K63 M1
Time 5 30 90 5 30 90 5 30 90 5 30 90 5 30 90 5 30 90 5 30 90 5 30 90 (min)
Ub2
Ub
d
K6
K63
K48
e
Lpg2529 7 325 572 OTU
Ub2 K6 K11 K27 K29 K33 K48 K63 M1
Time 5 30 90 5 30 90 5 30 90 5 30 90 5 30 90 5 30 90 5 30 90 5 30 90 (min)
Ub2
Ub
f
K63
K6
K48
K11
K33

Figure 2

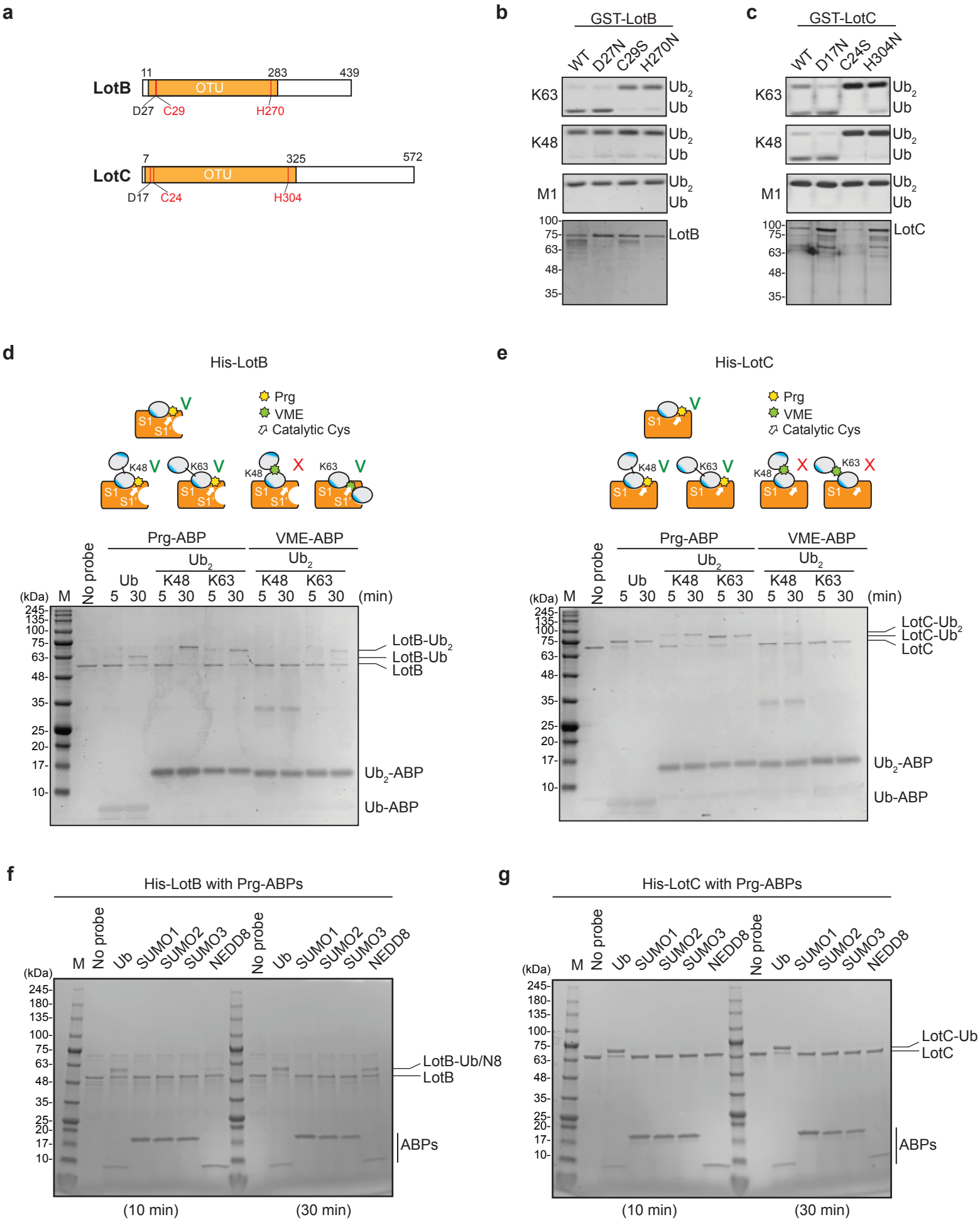
a
LotB
11
283
439
OTU
D27
C29
H270
LotC
7
325
572
OTU
D17
C24
H304
b
GST-LotB
WT
D27N
C29S
H270N
K63
K48
M1
Ub2
Ub
LotB
c
GST-LotC
WT
D17N
C24S
H304N
K63
K48
M1
Ub2
Ub
LotC
d
His-LotB
Prg
VME
Catalytic Cys
K48
K63
S1
S1'
Prg-ABP
VME-ABP
Ub2
No probe
Ub
K48
K63
(kDa)
M
5 30 5 30 5 30 5 30 5 30
(min)
LotB-Ub2
LotB-Ub
LotB
Ub2-ABP
Ub-ABP
e
His-LotC
Prg
VME
Catalytic Cys
K48
K63
S1
Prg-ABP
VME-ABP
Ub2
No probe
Ub
K48
K63
(kDa)
M
5 30 5 30 5 30 5 30 5 30
(min)
LotC-Ub2
LotC-Ub
LotC
Ub2-ABP
Ub-ABP
f
His-LotB with Prg-ABPs
M
No probe
Ub
SUMO1
SUMO2
SUMO3
NEDD8
No probe
Ub
SUMO1
SUMO2
SUMO3
NEDD8
(kDa)
LotB-Ub/N8
LotB
ABPs
(10 min)
(30 min)
g
His-LotC with Prg-ABPs
M
No probe
Ub
SUMO1
SUMO2
SUMO3
NEDD8
No probe
Ub
SUMO1
SUMO2
SUMO3
NEDD8
(kDa)
LotC-Ub
LotC
ABPs
(10 min)
(30 min)

Figure 3

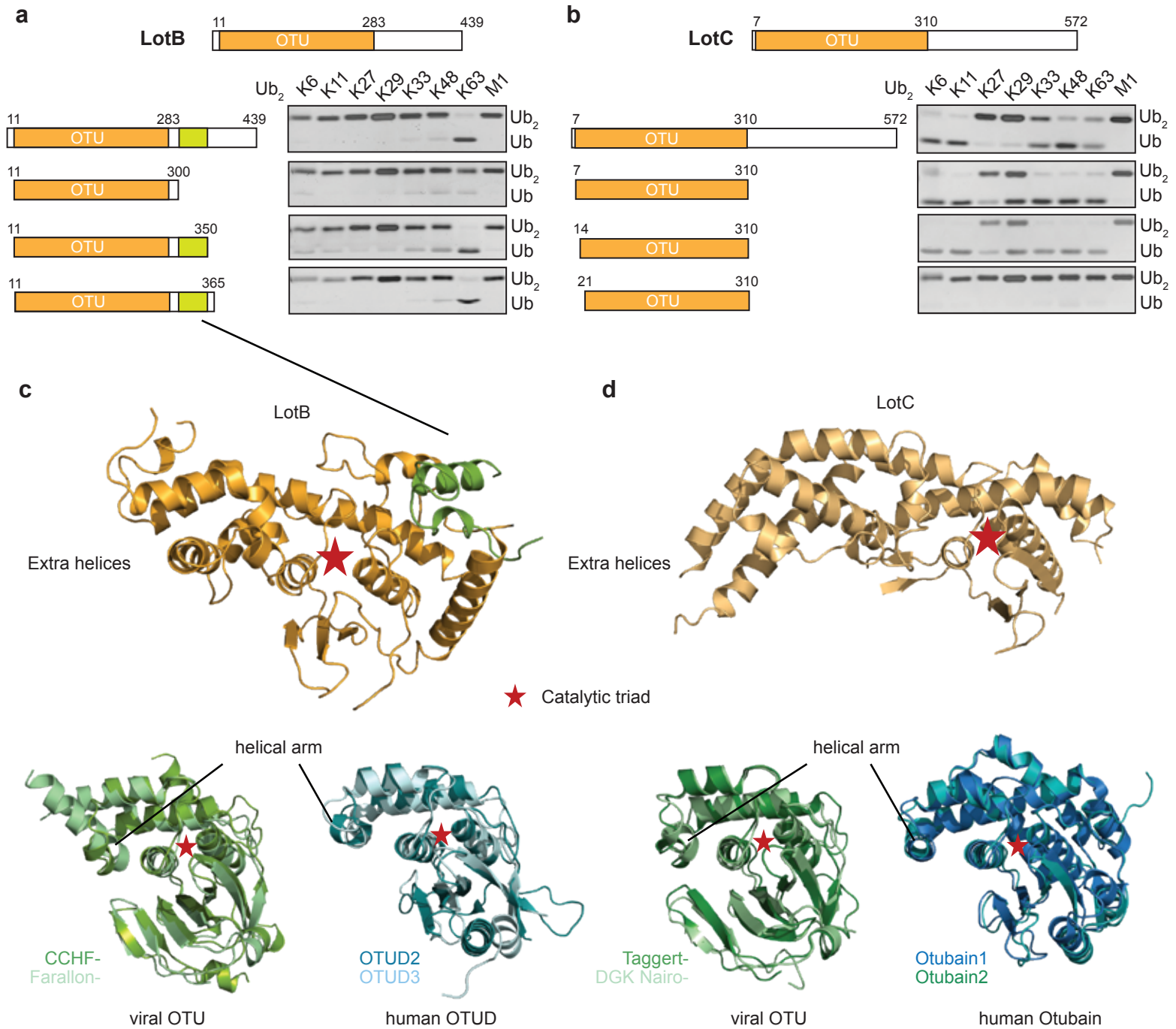

e

	Cys loop		Helical lobe		Variable loop		His loop	
LotB	SGAFDNC	29		213	LAKPQVKLSYI		IDALQGHY	271
vCCHF-OTU	QPGDGNC	40		94	LSDNEWGSTLE		LHSGQTHF	152
vFarallon-OTU	VKGDGNC	37		117	ATKEGYWGGTD		IVRCGAHF	175
hOTUD2	VPADNSC	160		213	IKRDDTWGGAI		LIYDGIHY	268
hOTUD3	VPGDGNC	76		127	LAKPGTFAGND		AYRYGEHY	183
LotC	NSGKGNC	24		235	LRREFVWGSEE		NNEGNVHW	305
vTaggert-OTU	QPMDGNC	40		93	IMKPNEWGSSL		IMHRRNHY	151
vDGK-OTU	VPGDGNC	42		94	LRNYYWGGSVE		LKLCQGHI	151
hOtubain1	TRPDGNC	91		208	VEPMCKESDHI		LLYRPGHY	266
hOtubain2	TKGDGNC	51		168	VEPMATECDHI		LLYKTSHY	225
LotA	ATGDGAC	13	Unknown structure	193	AFQRGYSCDEL		LENQEEHW	238
LotA	NPGLGNC	303	Unknown structure	482	ITQDFFWGTHL		TNSNNTHW	536

Figure 4

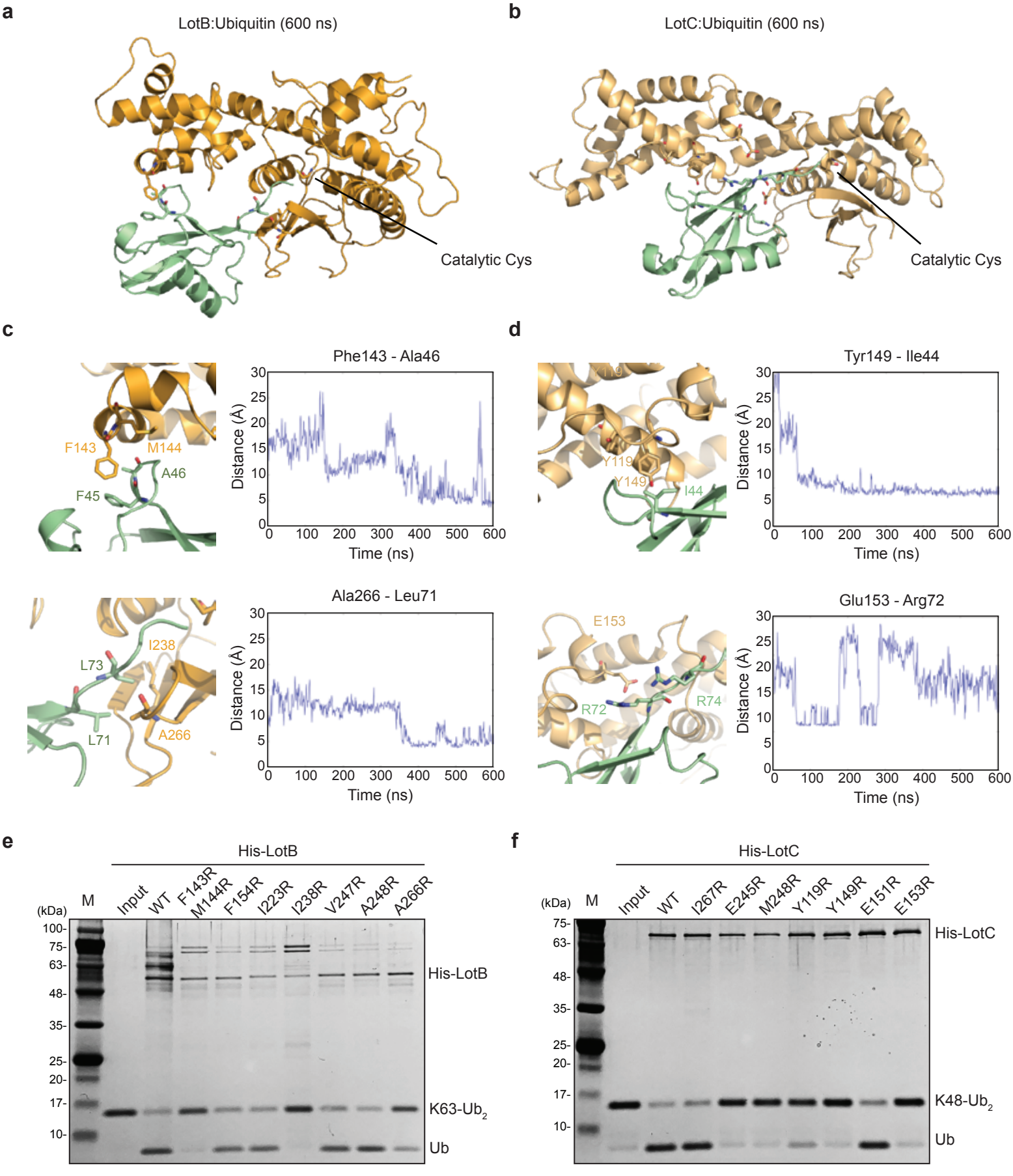
a
LotB:Ubiquitin (600 ns)
Catalytic Cys
b
LotC:Ubiquitin (600 ns)
Catalytic Cys
c
Phe143 - Ala46
F143
M144
A46
F45
Distance (Å)
Time (ns)
Ala266 - Leu71
I238
L73
L71
A266
d
Tyr149 - Ile44
Y119
Y149
I44
Glu153 - Arg72
E153
R72
R74
e
His-LotB
M
Input
WT
F143R
M144R
F154R
I223R
I238R
V247R
A248R
A266R
(kDa)
His-LotB
K63-Ub2
Ub
f
His-LotC
I267R
E245R
M248R
Y119R
Y149R
E151R
E153R
His-LotC
K48-Ub2
Ub

Figure 5

a

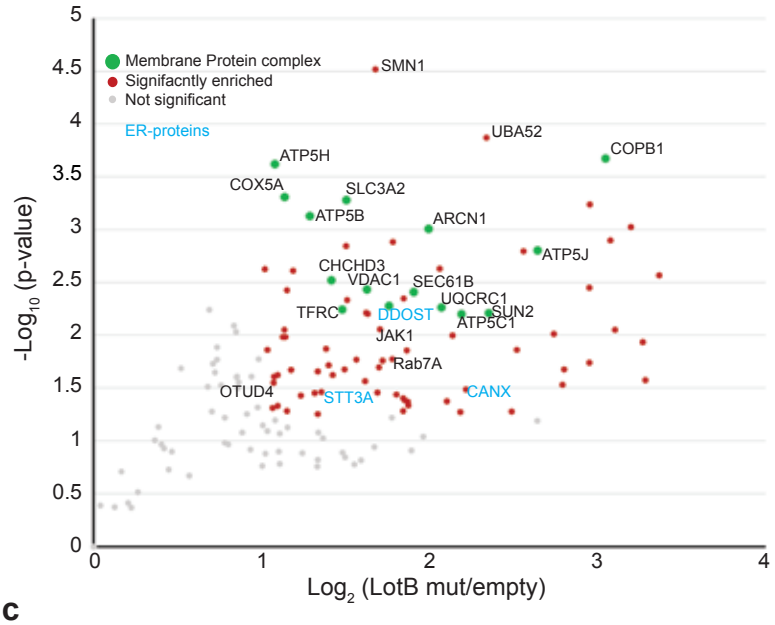

b

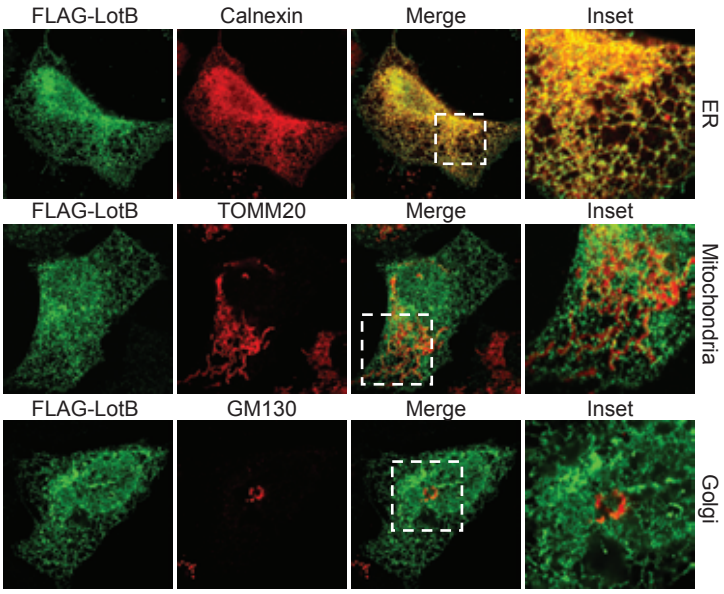

c

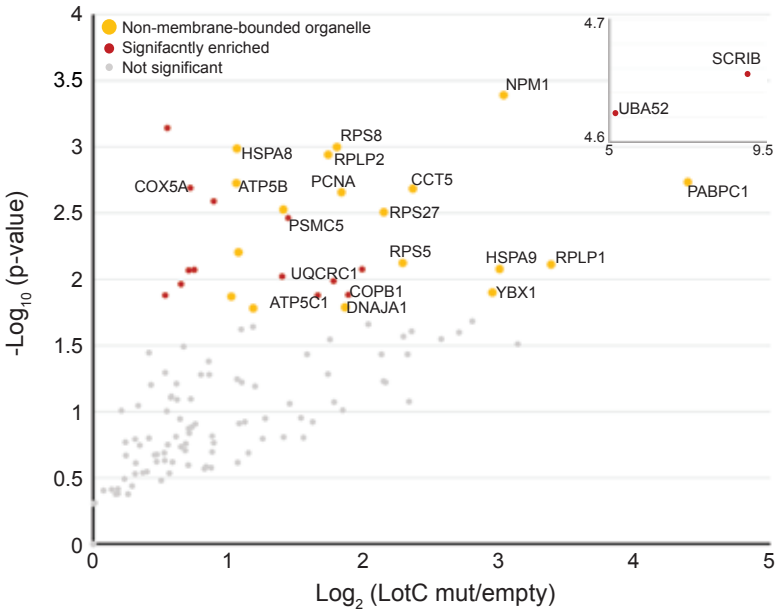

d

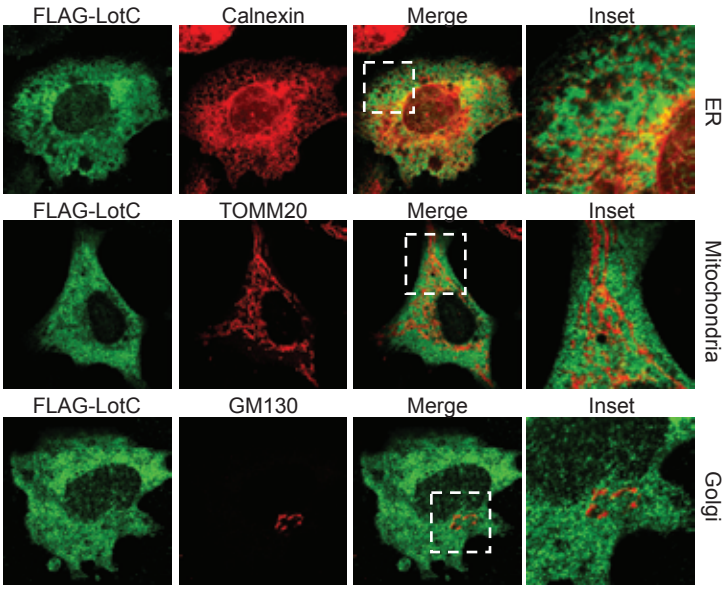

e

LotB-host proteins Interactome

without E3

Organelle

ARCN1	DOCK4	IPO8	SLC3A2
ATP1B3	EEF1A	JAK1	SMN1
BOLA2	EEF1D	KPNB1	SNRPD2
CANX	EMD	NONO	SRRM2
CCT3	GNB1	NPM1	STK38
CCT5	GOLGA3	OTUD4	STT3A
CKAP4	HDX	PABPC1	SUN2
CLNS1A	HNRNPC	PCNA	TCP1
CNOT1	HNRNPH1	PGRMC1	TFRC
COPB1	HNRNPK	PPIA	TMEM33
CSE1L	HNRNPM	PPM1B	TMPO
DDOST	HSPA8	PRDX1	TNRC6B
		PRKDC	TUBA1B
		PRMT5	TUBB
		PSMC3	TUBB2B
		PSMC5	WDR77
		PSMD4	
		PSPC1	C11orf84
		RAB11A	EIF3I
		RAB7A	ELMO2
		RIOK1	ERH
		RNF219	KPRP
		RPN1	PHGDH
		RPS18	PHKA1
		RPS27	PHKA2
		RPS5	PHKB
		RUVBL2	PHKG2
		SEC61B	UBA52

Mitochondrion

ATP5A1	HSPE1
ATP5B	LRRC59
ATP5C1	MYCBP
ATP5H	OGT
ATP5J	PHB
ATP5O	PHB2
BSG	SFXN1
CHCHD3	SLC25A5
COX5A	SLC25A6
CYB5R3	STOML2
DNAJA1	TUFM
HSPA1B	UQCRC1
HSPA9	VDAC1
HSPD1	

with SdcA

RPS9
EEF1D
HSP90AA1
SOD1
RPS14
CCT3
PPIA
HIST1H2B
ACTG1
GRAMD4
UBA52

with SidC

PSMC5
RUVBL1
RPS23
EEF1A
PSMD1
VPS33B

f

LotC-host proteins Interactome

without E3

Non-membrane-bounded organelle

HNRNPC	RPS5
NPM1	RPS8
EEF1D	RPS27
CCT5	PPM1B
RPLP1	PCNA
RPLP2	NONO
YBX1	DNAJA1
HSPA8	TUBA1B
HSPA9	PABPC1
TUBB	PABPC4
	ATP5B

SCRIB
UQCRC1
SLC3A2
COX5A
RBM10
ATP5H
COPB1
ATP5C1
PSMC5
PPIA
STK38
UBA52

with SdcA

Structural constituent of ribosome

		HSPA1B;1A
		PSMD1
RPL4	RPL29	DNAJA1
RPL5	RPL34	TCP1
RPL6	RPL35	RAB7A
RPL7	RPS2	RAB11A;B
RPL7A	RPS3A	STK38L
RPL8	RPS5	RBM39
RPL10	RPS6	PSMA4
RPL10A	RPS8	HIST1H
RPL11	RPS12	PSMC6
RPL13	RPS13	TRIM21
RPL18	RPS17	PHKB
RPL18A	RPS18	VDAC2
RPL23	RPS20	SUN2
RPL26	RPS25	RIOK1
RPL27	RPS26	PSMC1
RPL28	RPLP2	RPN1
	MRPL12	UBA52

with SidC

MRPL12	SERBP1
NDUFS4	NPM1
RPS12	SPTBN1
SF3B5	PRDX2
SLC25A1	UBA52

Supplementary Figure 1

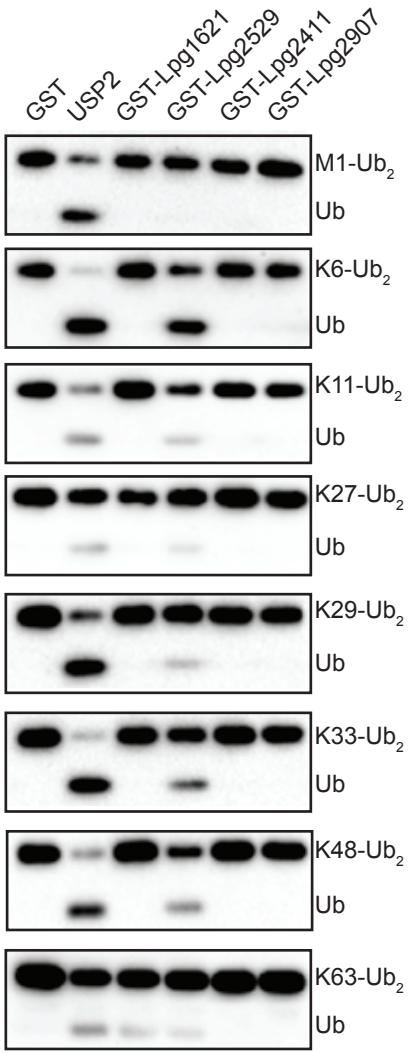

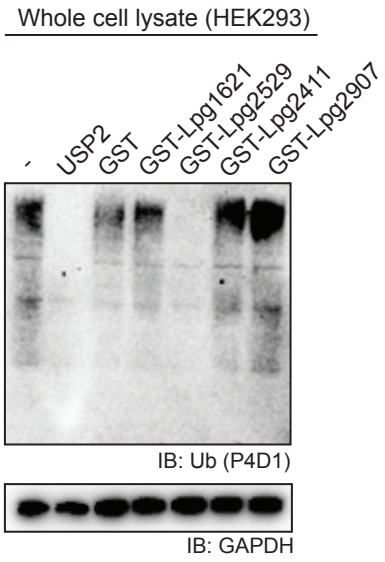

Supplementary Figure 2

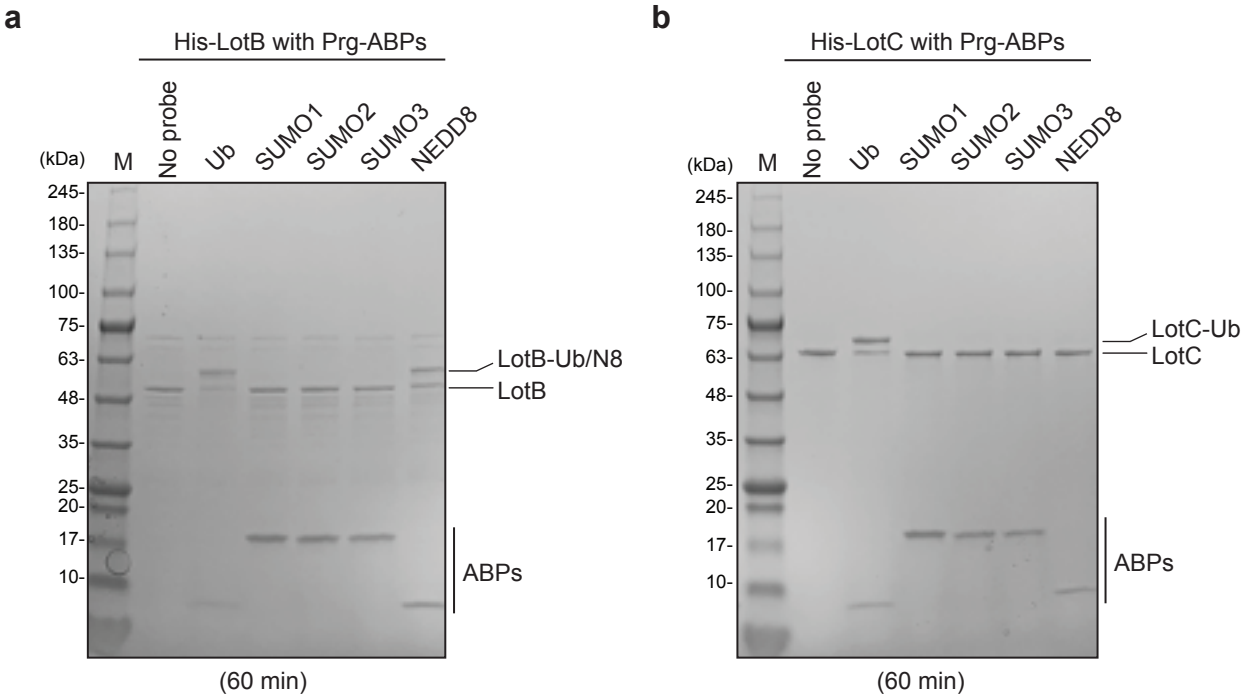

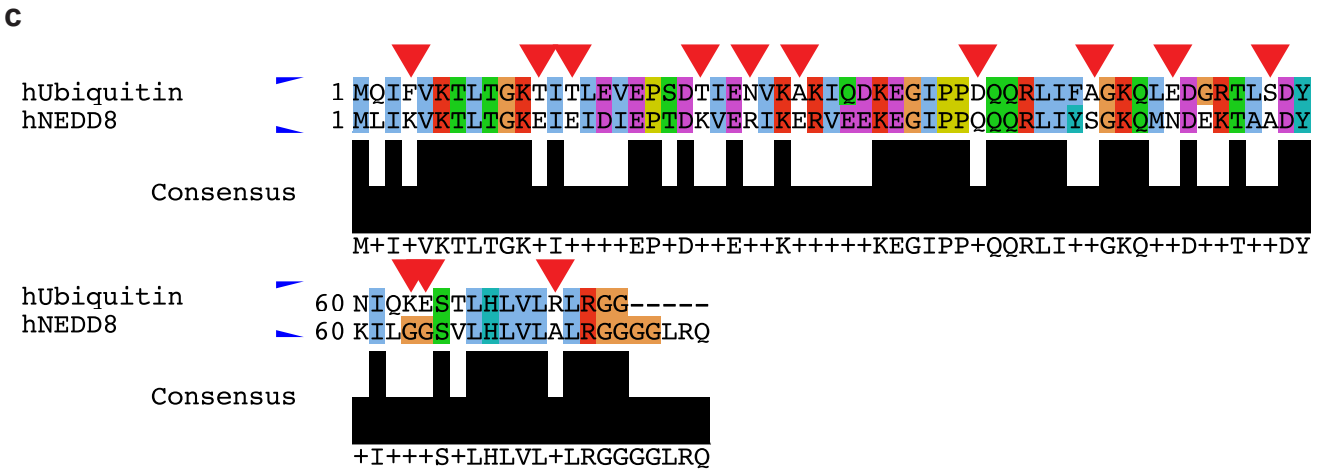

Supplementary Figure 3

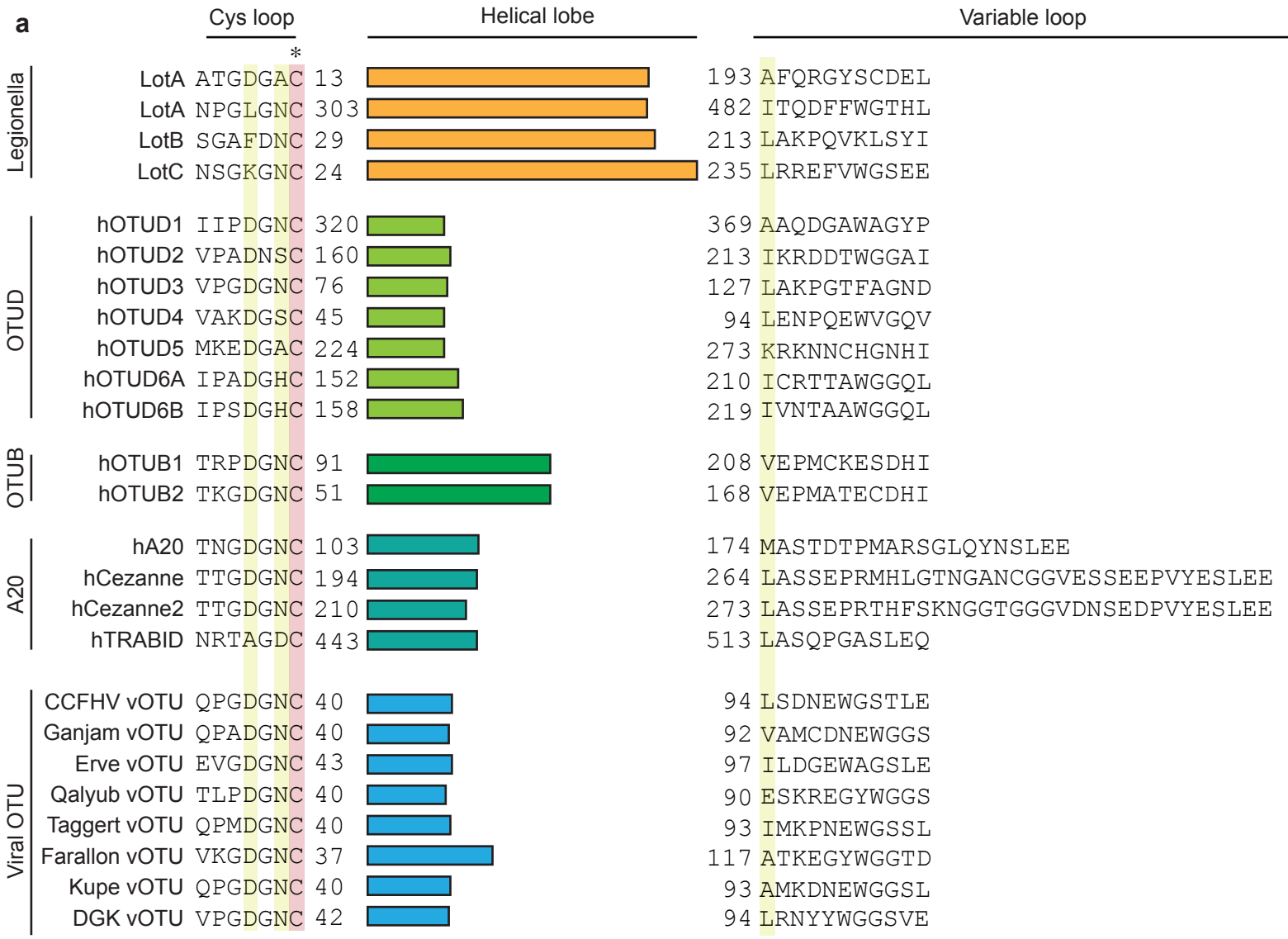

Supplementary Figure 4

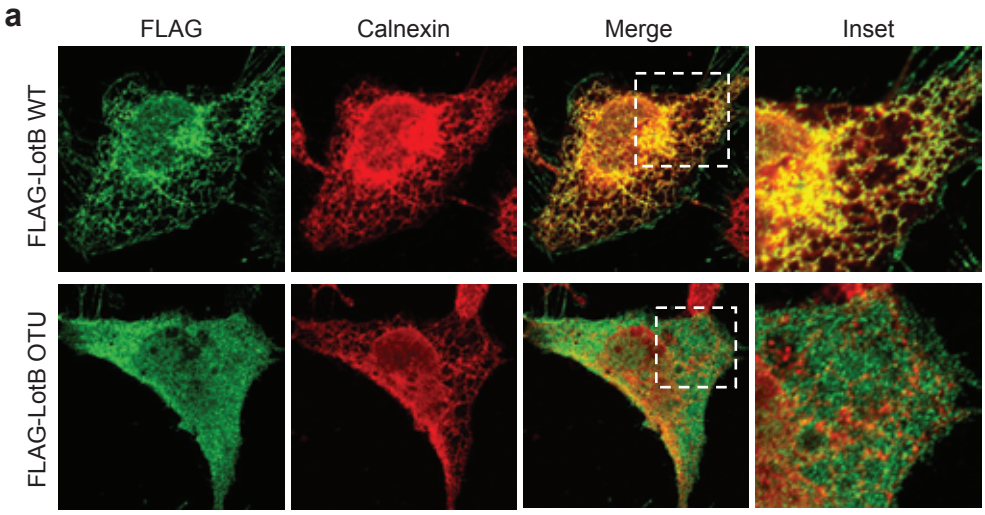

Supplementary Figure 5

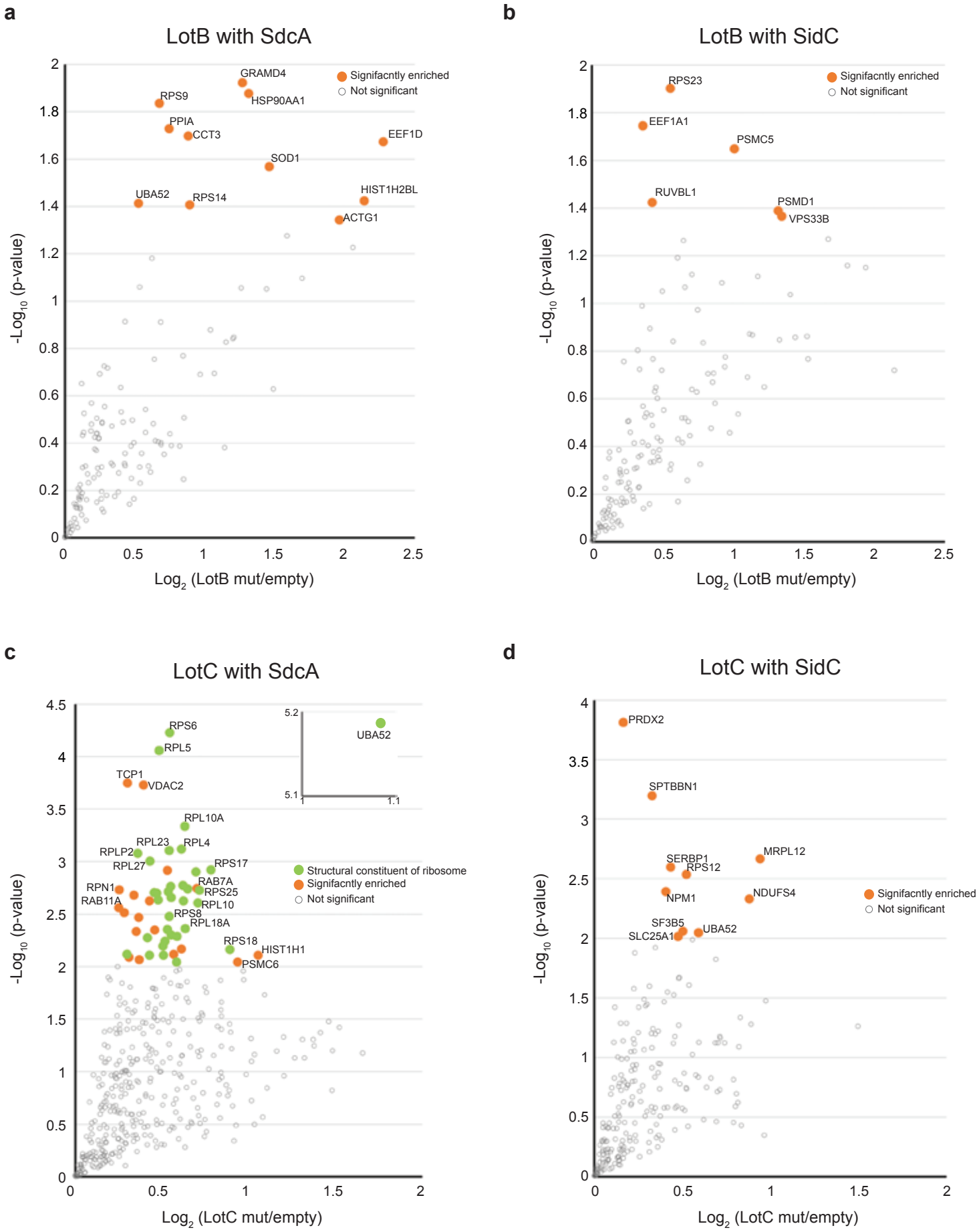

Supplmentary Figure 6 - Original blots

Fig. 1c; LotB Di-Ub2

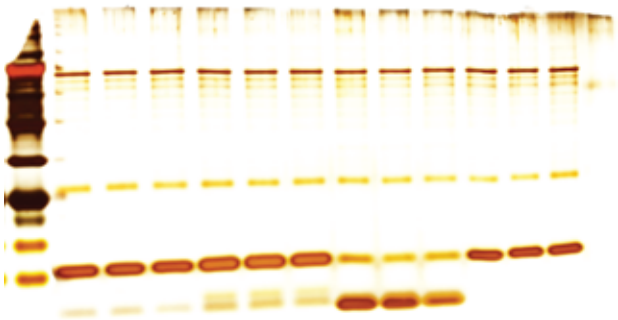

Fig. 1c; LotB Di-Ub2

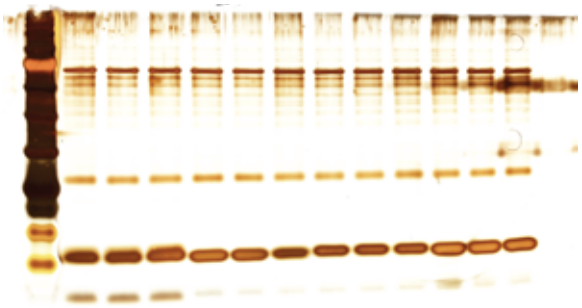

Fig. 1e; LotC Di-Ub2

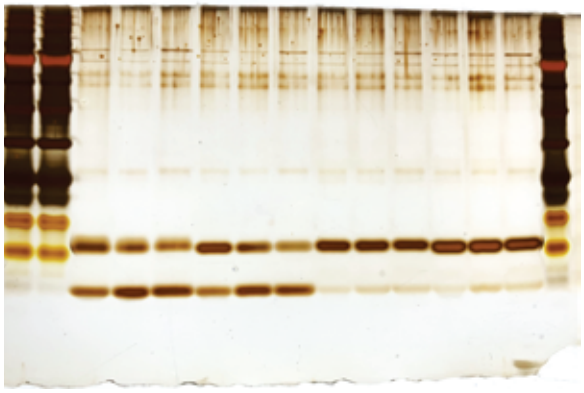

Fig. 1e; LotC Di-Ub2

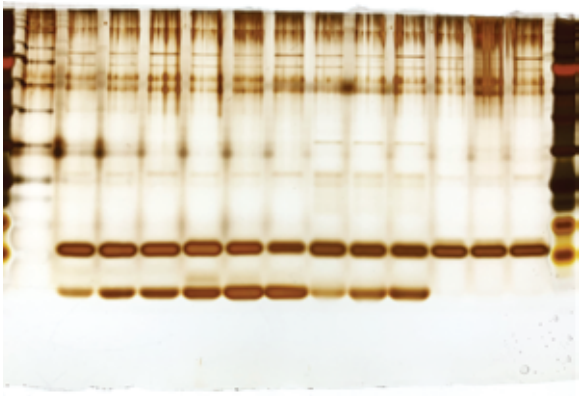

Fig. 2b; LotB catalytic muts

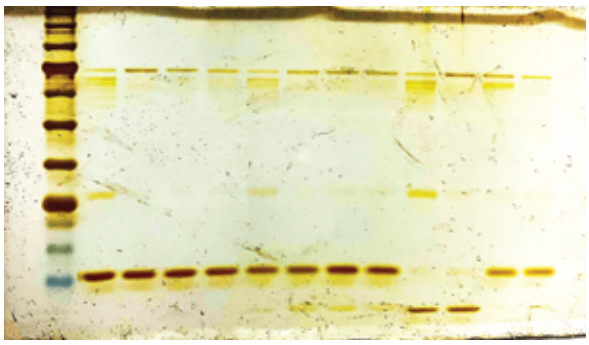

Fig. 2c; LotC catalytic muts

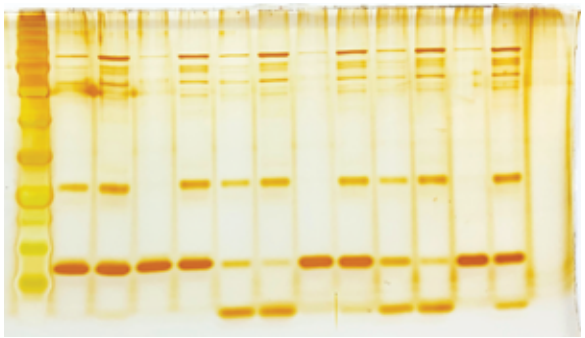

Fig. 2d; LotB ABP

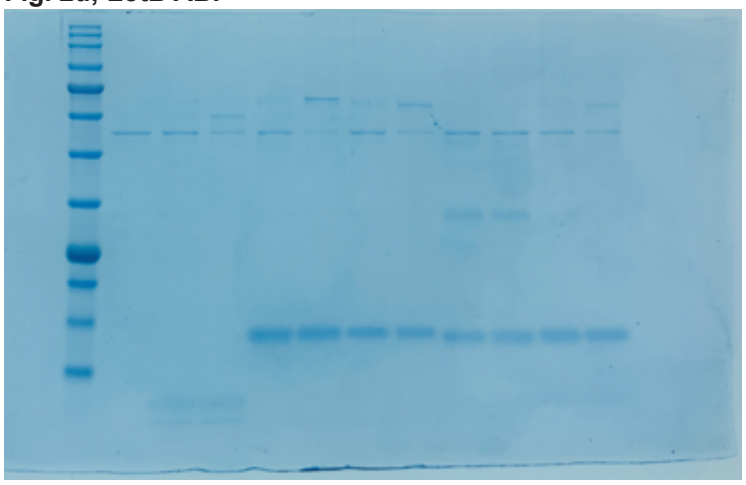

Fig. 2e; LotC ABP

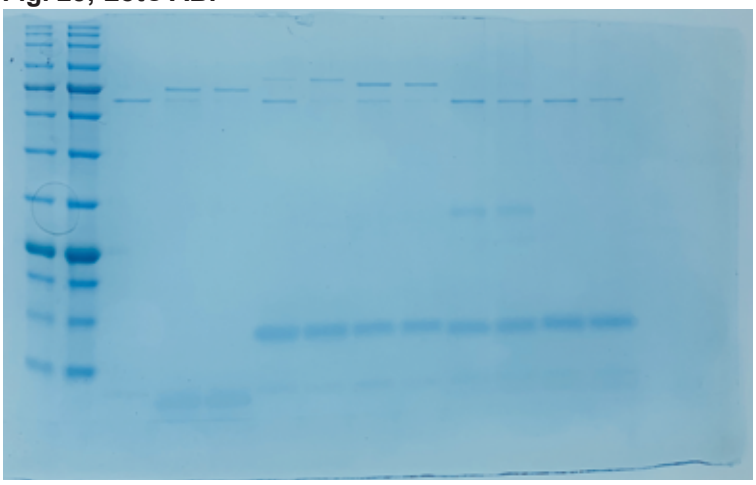

Fig. 2f; LotB ABP

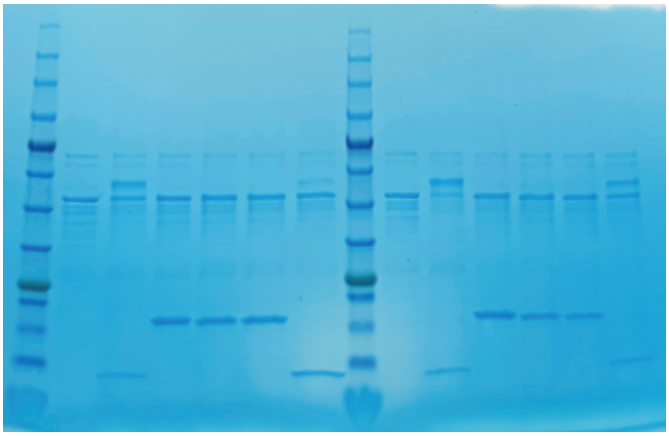

Fig. 2g; LotC ABP

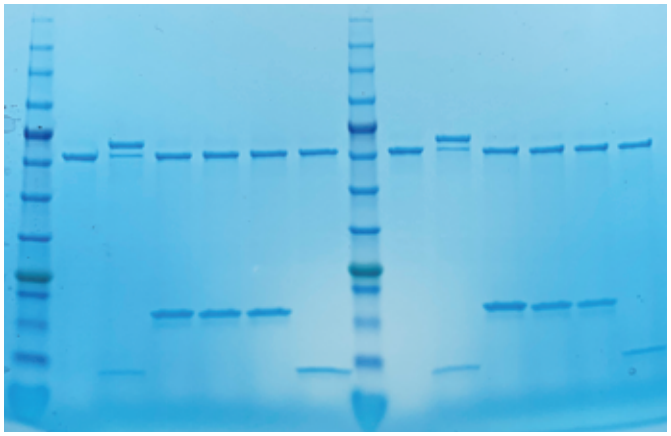

Sup Fig. 2a; LotB ABP

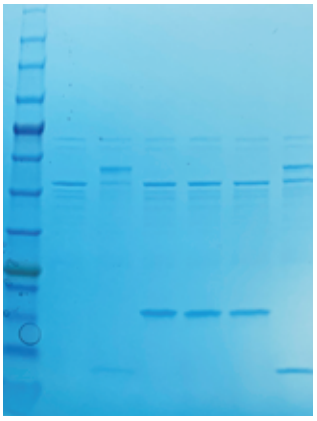

Sup Fig. 2b; LotB ABP

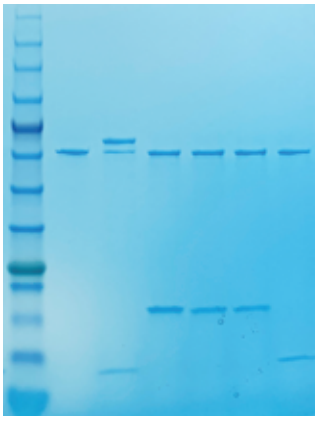

Fig. 3a; LotB WT

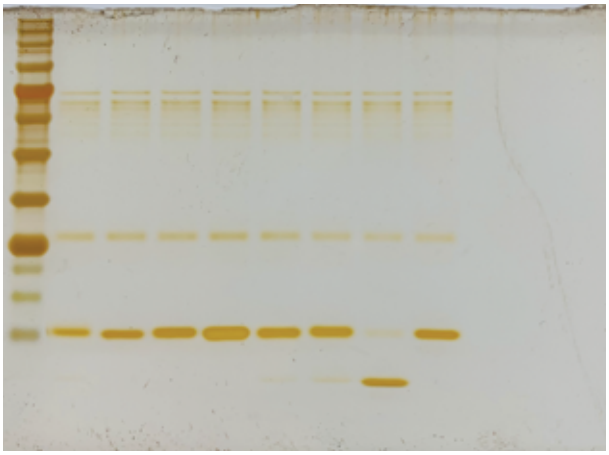

Fig. 3a; LotB 300

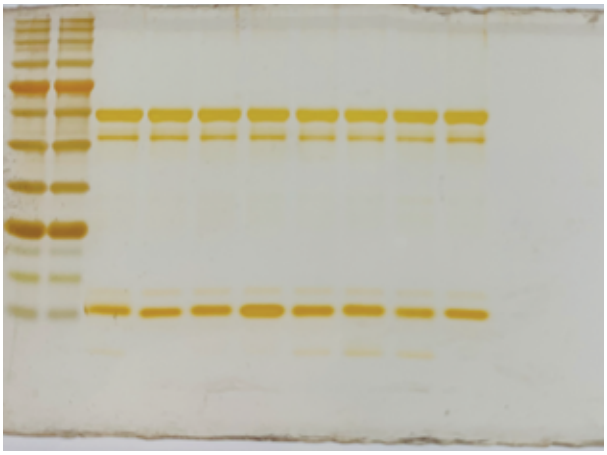

Fig. 3a; LotB 350

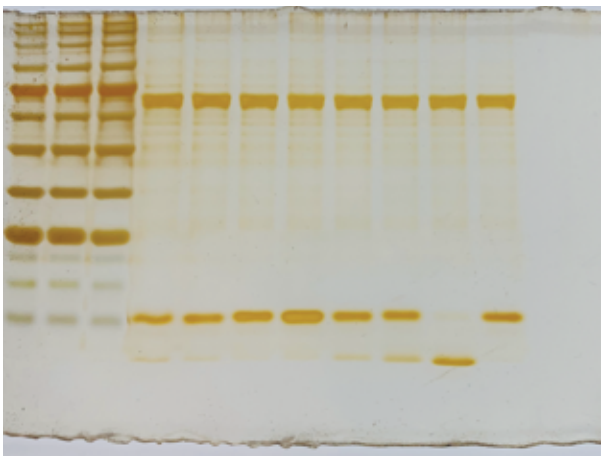

Fig. 3a; LotB 365

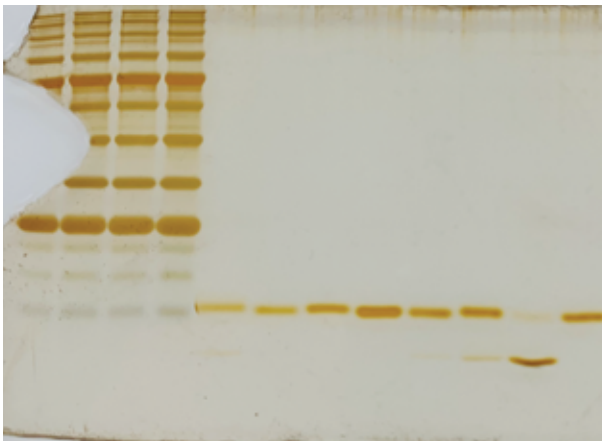

Fig. 3b; LotC WT

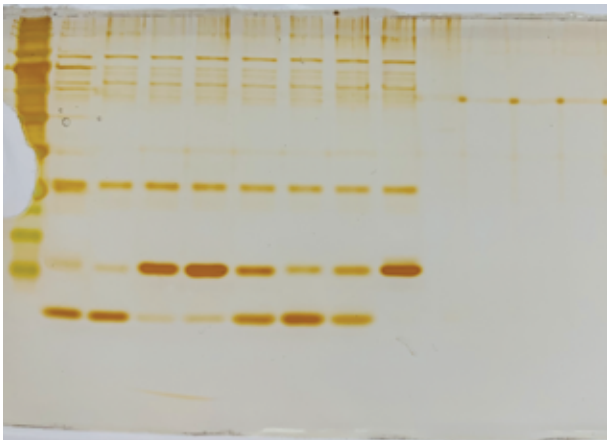

Fig. 3b; LotC 7

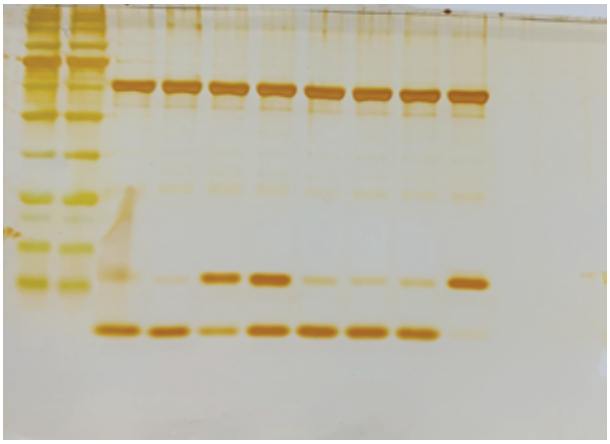

Fig. 3b; LotC 14

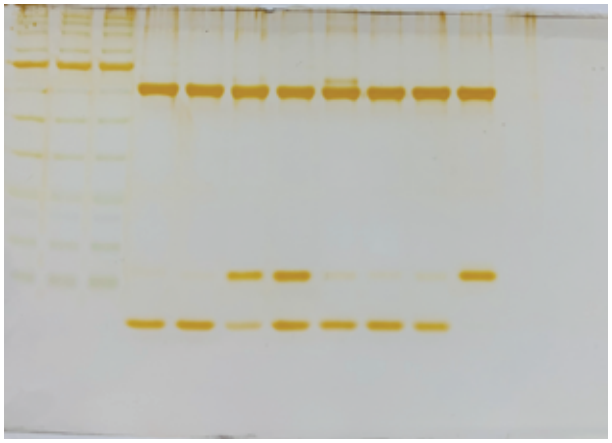

Fig. 3b; LotC 21

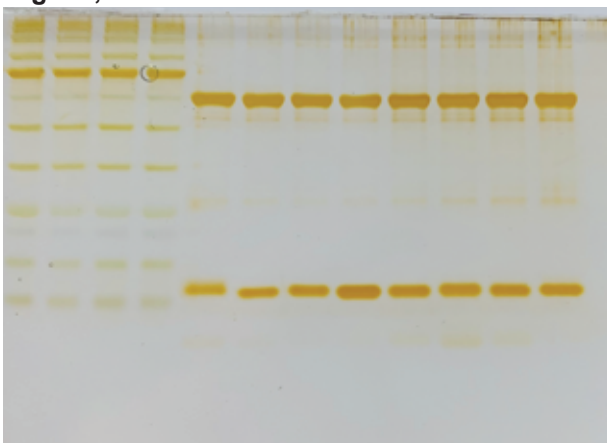

Fig. 4e; LotB mutants

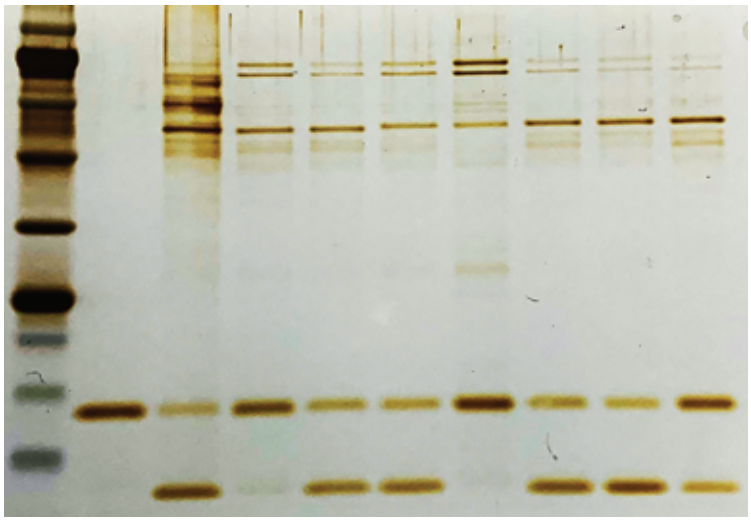
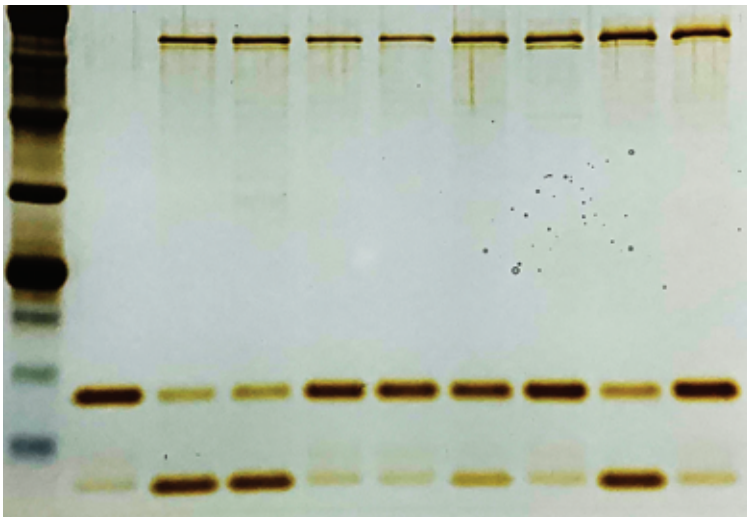
Fig. 4f; LotC mutants